

# Transport coefficients of hot and dense hadron gas in a magnetic field: A relaxation time approach

Arpan Das,<sup>1,\*</sup> Hiranmaya Mishra,<sup>1,†</sup> and Ranjita K. Mohapatra<sup>2,‡</sup>

<sup>1</sup>Theory Division, Physical Research Laboratory, Navrangpura, Ahmedabad 380009, India

<sup>2</sup>Department of Physics, Indian Institute of Technology Bombay, Mumbai 400076, India



(Received 26 September 2019; published 3 December 2019)

We estimate various transport coefficients of hot and dense hadronic matter in the presence of magnetic field. The estimation is done through solutions of the relativistic Boltzmann transport equation in the relaxation time approximation. We have investigated the temperature and the baryon chemical potential dependence of these transport coefficients. Explicit calculations are done for the hadronic matter in the ambit of hadron resonance gas model. We estimate thermal conductivity, electrical conductivity, and the shear viscosity of hadronic matter in the presence of a uniform magnetic field. Magnetic field, in general, makes the transport coefficients anisotropic. It is also observed that all the transport coefficients perpendicular to the magnetic field are smaller compared to their isotropic counterpart.

DOI: 10.1103/PhysRevD.100.114004

## I. INTRODUCTION

Strongly interacting matter produced in relativistic heavy-ion collision experiments at relativistic heavy ion collider (RHIC) and Large Hadron Collider (LHC) gives us a unique opportunity to study strong interaction in the nonperturbative regime. For a comprehensive understanding of the hot and dense QCD (quantum chromodynamics) medium produced in these experiments, transport coefficients play a crucial role. Large number of experimental data indicate the formation of quark-gluon plasma (QGP) in high multiplicity heavy-ion collision experiments. Quark-gluon plasma produced in the initial stage of heavy ion collision shows collective motion, undergoes subsequent space-time evolution and eventually gets chemically and thermally equilibrated, and results in a hadronic medium. Hydrodynamical modeling of the strongly interacting matter has been routinely used to study the transverse particle spectra of hadrons emanating out of the interaction region. In the context of hydrodynamical modeling, the dissipative effects can be important and the related transport coefficients, e.g., shear and bulk viscosity, etc., can play a significant role in this hydrodynamical evolution. In various literature, it has been argued that a small value of

shear viscosity to entropy density ratio ( $\eta/s$ ) can explain the flow data [1–3]. One of the remarkable achievements of the viscous hydrodynamical model is the prediction of a small value of  $\eta/s$  and perfect fluid behavior of the strongly interacting matter. A small value of  $\eta/s$  of the strongly coupled plasma produced in the heavy-ion collision is in accordance with the lower bound (Kovtun-Son-Starinets (KSS) bound) for the same,  $\eta/s = \frac{1}{4\pi}$  obtained using gauge gravity duality (AdS/CFT correspondence). Prediction of the small value of shear viscosity to entropy density ratio motivated a large number of investigations in understanding the microscopic origin of transport coefficients [3]. It is important to mention that KSS bound has been derived for a strongly coupled quantum field theory having conformal symmetry. However, QCD is not conformal and the deviation of the conformality is encoded in the bulk viscosity  $\zeta$  of the medium [4–12]. Bulk viscosity encodes the conformal measure  $(\epsilon - 3P)/T^4$  of the system, and lattice QCD simulations show a nonmonotonic behavior of both  $\eta/s$  and  $\zeta/s$  near the critical temperature  $T_c$ . [6–12]. Nonmonotonic behavior of bulk and shear viscosity is perhaps very natural because of the emergent scale, in this case,  $\Lambda_{\text{QCD}}$ , near the phase transition region.

Apart from the production of strongly interacting matter in a heavy-ion collision, generation of a nonvanishing electromagnetic field in the noncentral heavy-ion collisions allows one to study some novel interplay of quantum electrodynamics and QCD interactions. The strength of the magnetic field at the initial stages in these collisions can be large, at least of the order of several  $m_\pi^2$  at RHIC energies and may even be larger, i.e., of the order of  $15 m_\pi^2$  at LHC energies [13,14]. The presence of large external magnetic field can have nontrivial effects on the properties of QGP,

\* arpan@prl.res.in

† hm@prl.res.in

‡ ranjita@iitb.ac.in

Published by the American Physical Society under the terms of the Creative Commons Attribution 4.0 International license. Further distribution of this work must maintain attribution to the author(s) and the published article's title, journal citation, and DOI. Funded by SCOAP<sup>3</sup>.

as well as on the subsequent hadronic medium. This has motivated a large number of investigations on the properties of hot and dense matter under strong fields. Nontrivial nature of the QCD vacuum along with a strong magnetic field can give rise to novel CP (charge conjugation-parity) violating effects such as chiral magnetic effect [15]. Fluid dynamical behavior of the strongly interacting matter in the presence of magnetic field has been investigated within the framework of magnetohydrodynamic simulations [16,17]. To study the phenomenological manifestation of magnetic field on the strongly interacting matter, one requires the initial magnetic field to survive for at least a few Fermi proper time. The transport coefficient which plays the important role for the survival of magnetic field in a plasma is the electrical conductivity. In the magnetohydrodynamic limit, when the electrical conductivity of the medium is infinite, magnetic field is frozen in the plasma [16–34]. This apart thermal conductivity also plays a significant role in the hydrodynamical evolution [35,36]. Various approaches, e.g., perturbative QCD, different effective models, etc. have been used to estimate various transport coefficients of the QCD matter [37–66]. In the presence of constant magnetic field, the transport coefficients no longer remain isotropic. It can be shown that in the presence of magnetic field in general there can be five coefficients for shear viscosity, two coefficients bulk viscosity, and three coefficients for thermal conductivity [67]. In Ref. [67], for dissipative magnetohydrodynamics of strongly interacting medium, a complete set of transport coefficients, consistent with the Curie and Onsager principles, has been derived for thermal conduction, shear viscosity, and bulk viscosity. Further using Zubarevs nonequilibrium statistical operator method, Kubo formulas for these transport coefficients have been derived in Ref. [67].

In the present work, we investigate thermal conductivity, electrical conductivity, and shear viscosity for the hot and dense hadron gas produced in the subsequent evolution of QGP, in heavy-ion collisions, and in the presence of a magnetic field. In our previous works, we have investigated electrical conductivity and Hall conductivity for hot and dense hadronic matter [68] as well as for quark-gluon plasma [69]. It was shown that for strongly interacting medium, the electrical conductivity decreases in the presence of magnetic field while the Hall conductivity displays a nonmonotonic behavior with magnetic field. We had also pointed out that at zero baryon chemical potential Hall conductivity vanishes due to opposite gyration of particles and antiparticles. Only for nonvanishing baryon chemical potential, Hall conductivity has a finite value [70–73]. In these investigations, we had only considered the field configurations where the electric and the magnetic field are perpendicular to each other. In general, electric and magnetic field can have more general configurations. In the present investigation, we have considered a somewhat general configurations of electric and magnetic field.

For a general configuration of electric and magnetic field, we have calculated all the components of thermal conductivity, electrical conductivities, as well as shear viscosity. It is important to mention that the formalism that we use to calculate shear viscosity and electrical conductivity in the presence of magnetic field has been developed in Refs. [74–76]. The general configuration for the field leads to extra transport coefficients. As we shall show there are three different components for electrical and thermal conductivities and five components of shear viscosities. Some of the components for electrical conductivity vanish when the electric field and the magnetic field are perpendicular to each other [68,69]. In the present investigation, we study the effect of magnetic field on various transport coefficients of the hot and dense hadronic matter in a general electric and magnetic field configuration using the hadron resonance gas model within the framework of relaxation time approximation (RTA). It ought to be mentioned that a large magnetic field produced in the initial stage of heavy-ion collisions can be sustained in the medium with finite electrical conductivity. Some transport coefficients, e.g., bulk viscosity, thermal conductivity, etc. in the presence of magnetic field for the QGP phase using Landau quantization and considering only the lowest Landau level have been investigated in Refs. [77–80]. On the other hand, for the hadronic phase considered here, we limit ourselves to the case of small/moderate magnetic fields. Naturally, in such a case, while the equilibrium dynamics is decided by strong interaction, the effect of magnetic field is reflected through the cyclotron frequency of the individual hadrons. Such an approximation has been utilized earlier to estimate transport coefficients [76,81]. We will follow a similar approach for hadron resonance gas and naturally, the quantum effects due to Landau quantization are not included here.

The hadronic phase at chemical freeze-out can be described by well-celebrated hadron resonance gas (HRG) model [82,83]. To explain the experimental results of the thermal abundance of different hadron ratios in the heavy-ion collisions, HRG model has been successfully used [84]. Assuming a single chemical freeze-out surface of strange and nonstrange particles, HRG model can be described using only two parameters, temperature ( $T$ ) and baryon chemical potential ( $\mu_B$ ). Using S-matrix calculation, it has been shown that in the presence of narrow resonances, the thermodynamics of interacting gas of hadrons can be approximated by ideal gas of hadrons and its resonances [85,86]. Information of interaction among different hadrons has been encoded as the resonances. Due to this very simple description, HRG model has been well explored regarding thermodynamics [87,88], conserved charge fluctuations [89–94], as well as transport coefficients for hadronic matter [19,21,22,38–62]. Although many improvements have been done on ideal HRG model of noninteracting hadrons and its resonances,

e.g., including excluded volume HRG model [62,95], etc., in this investigation we confine ourselves to ideal HRG model for the estimation of various transport coefficients.

This paper is organized in the following manner. In Sec. II, we discuss the formalism of thermal conductivity in the presence of a magnetic field. In Secs. III and IV, we summarize the formalism to estimate electrical conductivity and shear viscosity in the presence of magnetic field. In Sec. V, we discuss salient feature of HRG model and summarize the formalism to calculate thermal averaged relaxation time. Then in Sec. VI, we present the results for thermal conductivity, electrical conductivity, and shear viscosity in the presence of magnetic field. Finally, we conclude our work with an outlook to it.

## II. THERMAL CONDUCTIVITY IN THE PRESENCE OF MAGNETIC FIELD

One of the important transport coefficients relevant for thermodynamic system with nonzero baryon density is the coefficient for thermal conductivity. Thermal conduction arises when energy flows relative to the baryonic enthalpy. Heat current of hadron resonance gas in the presence of conserved baryon current can be defined as [4]

$$\mathcal{I}^i = \sum_a T_a^{0i} - \frac{\omega}{n_B} \sum_a b_a j_B^i. \quad (1)$$

Here  $a$  is the particle index,  $b_a$  is the baryon number of different particles, e.g., for mesons  $b_{\text{meson}} = 0$ , for baryons  $b_{\text{baryon}} = 1$  and for antibaryons  $b_{\text{antibaryon}} = -1$ .  $\omega$  is the enthalpy of the system  $\omega = \mathcal{E} + P$ ,  $\mathcal{E}$  is the energy density of the system, and  $P$  is the pressure of the system. In Eq. (1),  $T^{\mu\nu}$  is the energy momentum tensor,  $j_B^\mu$  is the conserved baryon current, and  $n_B$  is the net number density of baryons. Using the standard definition of  $T^{\mu\nu}$  and  $j_B^\mu$ , heat current  $\mathcal{I}^i$  can be expressed as

$$\begin{aligned} \mathcal{I}^i &= \sum_a \int \frac{d^3 p_a}{(2\pi)^3} p_a^i f_a - \frac{\omega}{n_B} \sum_a b_a \int \frac{d^3 p_a}{(2\pi)^3} v_a^i f_a \\ &= \sum_a \int \frac{d^3 p_a}{(2\pi)^3} \frac{p_a^i}{\epsilon_a} \left( \epsilon_a - b_a \frac{\omega}{n_B} \right) \delta f_a. \end{aligned} \quad (2)$$

Here  $\epsilon_a = \sqrt{\vec{p}_a^2 + m_a^2}$  is the single particle dispersion relation, and  $\delta f_a = f_a - f_{0a}$  denotes deviation from equilibrium distribution function  $f_{0a} \equiv \frac{1}{e^{(\epsilon_a - \vec{p}_a \cdot \vec{u} - b_a \mu_B)/T} \pm 1}$ . The relativistic Boltzmann transport equation (RBTE) in the presence of a magnetic field of a single hadron species is given by [81]

$$\vec{v}_a \cdot \frac{\partial f_a}{\partial \vec{r}} + q_a (\vec{v}_a \times \vec{B}) \cdot \frac{\partial f_a}{\partial \vec{p}_a} = \mathcal{C}[f_a], \quad (3)$$

where  $q_a$  is the electric charge of the particle “a” and  $\mathcal{C}[f_a]$  is the collision integral. To study the transport coefficient, one is interested in small departure from equilibrium, i.e., one writes,  $f_a(\vec{x}, \vec{p}, t) = f_{0a} + \delta f_a$ . Substituting  $f_a$  in (3) and keeping linear terms in  $\delta f_a$ , we get [76]

$$\vec{v}_a \cdot \frac{\partial f_{0a}}{\partial \vec{r}} + q_a (\vec{v}_a \times \vec{B}) \cdot \frac{\partial (\delta f_a)}{\partial \vec{p}_a} = \mathcal{C}[\delta f_a]. \quad (4)$$

In the collision term, all the  $f_{0a}$  dependent terms vanish due to the principle of detailed balance while linear in  $\delta f_a$  term survives. In the lhs, of Eq. (3), we have used the relation  $\frac{\partial f_{0a}}{\partial \vec{p}_a} = \vec{v}_a \frac{\partial f_{0a}}{\partial \epsilon_a}$  and  $\vec{v} \cdot (\vec{v} \times \vec{B})$  contribution vanishes. Hence, we get Eq. (4) starting from Eq. (3) in the leading order approximation. In general, the collision integral can be complicated; however, in the RTA, the collision integral in the local rest frame takes simple form and it can be written as

$$\mathcal{C}[\delta f_a] \equiv -\frac{\delta f_a}{\tau_a}, \quad (5)$$

where  $\tau_a$  is the relaxation time which determines the timescale for the system to relax toward the equilibrium state characterized by the distribution function  $f_{0a}$ . The underlying assumption of the relaxation time approximation is that the system is slightly away from equilibrium due to external perturbation and then it relaxes toward equilibrium with the timescale  $\tau_a$ . In relaxation time approximation, external perturbation is not the dominant scale. In the strongly interacting medium, strong interaction is responsible for thermalization of the medium and the external electromagnetic field is a perturbation with respect to the strong dynamics. The equilibrium distribution function satisfies

$$\begin{aligned} \frac{\partial f_{0a}}{\partial \vec{p}_a} &= \vec{v}_a \frac{\partial f_{0a}}{\partial \epsilon_a}, & \frac{\partial f_{0a}}{\partial \epsilon_a} &= -\beta f_{0a} (1 \mp f_{0a}), \\ f_{0a} &= \frac{1}{e^{(\epsilon_a - \vec{p}_a \cdot \vec{u} - b_a \mu_B)/T} \pm 1}, \end{aligned} \quad (6)$$

where the single particle energy is  $\epsilon_a(p_a) = \sqrt{\vec{p}_a^2 + m_a^2}$ ,  $\mu_B$  is the baryon chemical potential, and  $\beta = 1/T$  is the inverse of temperature.  $\vec{v}_a = \vec{p}_a/\epsilon_a$  is the velocity of the particle,  $\vec{u}$  is the fluid velocity. In the local rest frame,  $\vec{u} = 0$ .  $\pm$  is for fermion and boson, respectively. In the presence of temperature gradient and magnetic field, we can express deviation of distribution function from the equilibrium in the following way [75]:

$$\delta f_a = (\vec{p}_a \cdot \vec{\Xi}) \frac{\partial f_{0a}}{\partial \epsilon_a}, \quad (7)$$

with  $\vec{\Xi}$  being related to temperature gradient, the magnetic field, and in general can be written as

$$\vec{\Xi} = \alpha \vec{\nabla} T + b \vec{h} + c (\vec{\nabla} T \times \vec{h}), \quad (8)$$

where  $\vec{h} = \frac{\vec{B}}{B}$  is the direction of the magnetic field. Using  $\delta f$  as given in Eq. (7), Eq. (4) can be expressed as

$$-q_a B \vec{v}_a \cdot (\vec{\Xi} \times \vec{h}) \frac{\partial f_{0a}}{\partial \epsilon_a} + \vec{v}_a \cdot \vec{\nabla} f_{0a} = -\frac{\epsilon_a}{\tau_a} (\vec{v}_a \cdot \vec{\Xi}) \frac{\partial f_{0a}}{\partial \epsilon_a}. \quad (9)$$

Here,

$$\vec{\nabla} f_{0a} = T \frac{\partial f_{0a}}{\partial \epsilon_a} \left[ \epsilon_a \vec{\nabla} \left( \frac{1}{T} \right) - b_a \vec{\nabla} \left( \frac{\mu_B}{T} \right) \right]. \quad (10)$$

Using Gibbs-Duhem relation for the steady state  $\vec{\nabla} P = \omega \frac{\vec{\nabla} T}{T} + n_B T \vec{\nabla} (\mu_B/T) = 0$ , we get [4]

$$\vec{\nabla} f_{0a} = -\frac{\partial f_{0a}}{\partial \epsilon_a} \left( \epsilon_a - b_a \frac{\omega}{n_B} \right) \frac{\vec{\nabla} T}{T}. \quad (11)$$

It ought to be mentioned that in the presence of magnetic field first law of thermodynamics as well as Gibbs-Duhem relation can get modified. However, this modification involves magnetization of the system. In this present investigation, we are not considering magnetization of the system. Using Eq. (11) and the representation of  $\vec{\Xi}$  as given in Eq. (8), Eq. (9) can be expressed as

$$\begin{aligned} & -q_a B \alpha \vec{v}_a \cdot (\vec{\nabla} T \times \vec{h}) - q_a B c (\vec{v}_a \cdot \vec{h}) (\vec{\nabla} T \cdot \vec{h}) + q_a B c (\vec{v}_a \cdot \vec{\nabla} T) \\ & - \left( \epsilon_a - b_a \frac{\omega}{n_B} \right) \vec{v}_a \cdot \vec{\nabla} \ln T \\ & = -\frac{\epsilon_a}{\tau_a} [\alpha \vec{v}_a \cdot \vec{\nabla} T + b (\vec{v}_a \cdot \vec{h}) + c \vec{v}_a \cdot (\vec{\nabla} T \times \vec{h})]. \end{aligned} \quad (12)$$

Comparing coefficients of different tensor structures in Eq. (12), we get

$$c = \frac{q_a B}{\epsilon_a} \tau_a \alpha \equiv \omega_{c_a} \tau_a \alpha, \quad (13)$$

$$b = (\omega_{c_a} \tau_a)^2 \alpha (\vec{\nabla} T \cdot \vec{h}) \quad (14)$$

and

$$q_a B c - \frac{\epsilon_a - b_a \frac{\omega}{n_B}}{T} = -\frac{\epsilon_a \alpha}{\tau_a}. \quad (15)$$

Here  $\omega_{c_a} = \frac{q_a B}{\epsilon_a}$  is the cyclotron frequency of the particle with electric charge  $q_a$ . Using Eqs. (13)–(15), it can be shown that

$$\alpha = \left( \frac{\tau_a}{\epsilon_a} \right) \left( \frac{\epsilon_a - b_a \frac{\omega}{n_B}}{T} \right) \frac{1}{1 + (\omega_{c_a} \tau_a)^2}. \quad (16)$$

Hence, the deviation of distribution function from equilibrium is

$$\begin{aligned} \delta f_a &= \frac{\tau_a (\epsilon_a - b_a \frac{\omega}{n_B})}{1 + (\omega_{c_a} \tau_a)^2} [\vec{v}_a \cdot \vec{\nabla} \ln T + (\omega_{c_a} \tau_a) \vec{v}_a \cdot (\vec{\nabla} \ln T \times \vec{h}) \\ &+ (\omega_{c_a} \tau_a)^2 (\vec{v}_a \cdot \vec{h}) (\vec{\nabla} \ln T \cdot \vec{h})] \frac{\partial f_{0a}}{\partial \epsilon_a}. \end{aligned} \quad (17)$$

With the deviation  $\delta f^a$  for the distribution function as above known from RBTE, the heat current as given in Eq. (4) can be expressed as

$$\begin{aligned} T^i &= \sum_a \frac{\tau_a}{T} \int d^3 p_a \frac{p_a^i p_a^j (\epsilon_a - b_a \frac{\omega}{n_B})^2}{\epsilon_a^2 1 + (\omega_{c_a} \tau_a)^2} \\ &\quad \times (\nabla^j T + (\omega_{c_a} \tau_a) \epsilon^{jkl} \nabla^k T h^l + (\omega_{c_a} \tau_a)^2 h^i h^l \nabla^l T) \frac{\partial f_{0a}}{\partial \epsilon_a} \\ &= \sum_a \frac{\tau_a}{3T} \int d^3 p_a \frac{p_a^2 (\epsilon_a - b_a \frac{\omega}{n_B})^2}{\epsilon_a^2 1 + (\omega_{c_a} \tau_a)^2} \\ &\quad \times (\delta^{ik} - (\omega_{c_a} \tau_a) \epsilon^{ilk} h^l + (\omega_{c_a} \tau_a)^2 h^i h^k) \nabla^l T \frac{\partial f_{0a}}{\partial \epsilon_a} \\ &= -(k_0 \delta^{ik} - k_1 \epsilon^{ilk} h^l + k_2 h^i h^k) \nabla^k T. \end{aligned} \quad (18)$$

Here we have introduced the different components of the thermal conductivity  $k_0$ ,  $k_1$ , and  $k_2$ . In Boltzmann approximation, these coefficients are explicitly given as, respectively,

$$k_0 = \sum_a \frac{g_a}{3T^2} \int \frac{d^3 p_a}{(2\pi)^3} \left( \frac{p_a^2}{\epsilon_a^2} \right) \frac{(\epsilon_a - b_a \frac{\omega}{n_B})^2}{1 + (\omega_{c_a} \tau_a)^2} f_{0a} \tau_a, \quad (19)$$

$$k_1 = \sum_a \frac{g_a}{3T^2} \int \frac{d^3 p_a}{(2\pi)^3} \left( \frac{p_a^2}{\epsilon_a^2} \right) \frac{(\epsilon_a - b_a \frac{\omega}{n_B})^2 (\omega_{c_a} \tau_a)}{1 + (\omega_{c_a} \tau_a)^2} f_{0a} \tau_a, \quad (20)$$

$$k_2 = \sum_a \frac{g_a}{3T^2} \int \frac{d^3 p_a}{(2\pi)^3} \left( \frac{p_a^2}{\epsilon_a^2} \right) \frac{(\epsilon_a - b_a \frac{\omega}{n_B})^2 (\omega_{c_a} \tau_a)^2}{1 + (\omega_{c_a} \tau_a)^2} f_{0a} \tau_a. \quad (21)$$

Here  $\epsilon_a$ ,  $g_a$ ,  $\tau_a$  are the single particle dispersion relation, degeneracy factor, and relaxation time of ‘‘a’’th particle species. From Eq. (19), it is clear that for nonvanishing magnetic field thermal conductivity gets modified. It may be noted that in the absence of the magnetic field, the coefficients  $k_1$  and  $k_2$  vanish and the thermal conductivity becomes isotropic and is given by the coefficient  $k_0$ . Further  $k_2$  and  $k_1$  are associated with  $\vec{\nabla} T \cdot \vec{h}$  and  $\vec{\nabla} T \times \vec{h}$

terms in the expression of  $\delta f_a$ . Hence, if  $\vec{\nabla}T$  is perpendicular to  $\vec{B}$ , then  $k_2$  vanishes and there are two nonvanishing coefficients of the thermal conductivity  $k_0$  and  $k_1$ . For a general configuration of temperature gradient and magnetic field,  $\vec{\nabla}T \cdot \vec{h}$  can be nonzero; hence, in that case, all the three components  $k_0$ ,  $k_1$ , and  $k_2$  are nonvanishing. We may point out that in the absence of magnetic field the expression of  $k_0$  as given in Eq. (19) can also be derived systematically as shown in Refs. [96,97] in the Landau frame where the flow velocity is identified with the energy flow rather than baryon number flow as in the Eckert frame.

### III. ELECTRICAL CONDUCTIVITY IN THE PRESENCE OF MAGNETIC FIELD

Similar to thermal conductivity, to calculate electrical conductivity, we start with the RBTE of single hadron species in the presence of external electromagnetic field [81],

$$p^\mu \partial_\mu f + qF^{\mu\nu} p_\nu \frac{\partial f}{\partial p^\mu} = \mathcal{C}[f]. \quad (22)$$

Here  $q$  is the electric charge of the particle,  $p^\mu$  is the particle four momenta,  $F^{\mu\nu}$  is the electromagnetic field strength tensor, and  $\mathcal{C}[f]$  is the collision integral. For a static and homogeneous case, in relaxation time approximation, we can write the kinetic equation as given in Eq. (22) as an equation for deviation from equilibrium  $\delta f = f - f_0$  [76],

$$q\vec{E} \cdot \frac{\partial f_0}{\partial \vec{p}} + q(\vec{v} \times \vec{B}) \cdot \frac{\partial(\delta f)}{\partial \vec{p}} = \mathcal{C}[\delta f] \equiv -\frac{\delta f}{\tau}. \quad (23)$$

In the presence of electric and magnetic field, we can take an ansatz for the deviation of the equilibrium distribution function in the following way [75]:

$$\delta f = (\vec{p} \cdot \vec{\Xi}) \frac{\partial f_0}{\partial \epsilon}, \quad (24)$$

with

$$\vec{\Xi} = a\vec{e} + b\vec{h} + c(\vec{e} \times \vec{h}), \quad (25)$$

where  $\vec{e} = \frac{\vec{E}}{|\vec{E}|}$  and  $\vec{h} = \frac{\vec{B}}{|\vec{B}|}$  are the direction of the electric field and magnetic field, respectively. This is similar to the ansatz taken as in Eq. (7) for the calculation of thermal conductivity, with  $\vec{\nabla}T$  now being replaced by  $\vec{e}$ . Using Eqs. (24) and (25), Eq. (23) can be expressed as

$$\begin{aligned} q(\vec{E} \cdot \vec{v}) - qBa\vec{v} \cdot (\vec{e} \times \vec{h}) - qBc(\vec{e} \cdot \vec{h})(\vec{v} \cdot \vec{h}) + qBc(\vec{v} \cdot \vec{e}) \\ = -\frac{\epsilon}{\tau} [a(\vec{v} \cdot \vec{e}) + b(\vec{v} \cdot \vec{h}) + c\vec{v} \cdot (\vec{e} \times \vec{h})]. \end{aligned} \quad (26)$$

Comparing coefficients of difference tensor structures in Eq. (26), we get

$$c = \frac{qB}{\epsilon} \tau a \equiv \omega_c \tau a, \quad (27)$$

$$b = (\omega_c \tau)^2 a (\vec{e} \cdot \vec{h}) \quad (28)$$

and

$$qBc + qE = -\frac{\epsilon a}{\tau}. \quad (29)$$

Using Eqs. (27)–(29), it can be shown that

$$a = \frac{-qE}{1 + (\omega_c \tau)^2} \left( \frac{\tau}{\epsilon} \right). \quad (30)$$

Hence,

$$\begin{aligned} \delta f = -\frac{q\tau}{1 + (\omega_c \tau)^2} \\ \times [\vec{v} \cdot \vec{E} + (\omega_c \tau) \vec{v} \cdot (\vec{E} \times \vec{h}) + (\omega_c \tau)^2 (\vec{v} \cdot \vec{h})(\vec{E} \cdot \vec{h})] \frac{\partial f_0}{\partial \epsilon}. \end{aligned} \quad (31)$$

The electric current ( $\vec{j}$ ) can be defined as

$$\vec{j} = \int \frac{d^3 p}{(2\pi)^3} q \vec{v} \delta f. \quad (32)$$

Using Eq. (31), electric current as given in Eq. (32) can be expressed as

$$\begin{aligned} j^i = \frac{q^2}{3} \int \frac{d^3 p}{(2\pi)^3} \frac{v^2 \tau}{1 + (\omega_c \tau)^2} \\ \times [E^i + (\omega_c \tau) \epsilon^{ijk} h^k E^j + (\omega_c \tau)^2 h^i h^j E^j] \left( -\frac{\partial f_0}{\partial \epsilon} \right) \\ = (\sigma_0 \delta^{ij} - \sigma_1 \epsilon^{ljk} h^k + \sigma_2 h^i h^j) E^j. \end{aligned} \quad (33)$$

From Eq. (33), we can identify various components of electrical conductivity tensor in the presence of magnetic field,

$$\sigma_0 = \frac{q^2}{3T} \int \frac{d^3 p}{(2\pi)^3} \tau \left( \frac{p^2}{\epsilon^2} \right) \frac{1}{1 + (\omega_c \tau)^2} f_0, \quad (34)$$

$$\sigma_1 = \frac{q^2}{3T} \int \frac{d^3 p}{(2\pi)^3} \tau \left( \frac{p^2}{\epsilon^2} \right) \frac{\omega_c \tau}{1 + (\omega_c \tau)^2} f_0, \quad (35)$$

$$\sigma_2 = \frac{q^2}{3T} \int \frac{d^3 p}{(2\pi)^3} \tau \left( \frac{p^2}{\epsilon^2} \right) \frac{(\omega_c \tau)^2}{1 + (\omega_c \tau)^2} f_0. \quad (36)$$

It is important to note that in Refs. [68,69] we discussed electrical conductivity and Hall conductivity in the presence of magnetic field.  $\sigma_0$  and  $\sigma_1$  as given in Eqs. (34) and (35) can be identified with electrical conductivity in the

presence of magnetic field and Hall conductivity, respectively, as obtained in Ref. [68]. In Refs. [68,69], we only considered electric field and magnetic field perpendicular to each other; however, for a general configuration of electric and magnetic field, we get another transport coefficient  $\sigma_2$  [75]. Hence, for a general configurations of electric and magnetic field, we have three different components of electrical conductivity tensor. For a multi-component model, total  $\sigma_0$ ,  $\sigma_1$ , and  $\sigma_2$  can be expressed as

$$\sigma_0 = \sum_i \frac{q_i^2 g_i}{3T} \int \frac{d^3 p}{(2\pi)^3} \left( \frac{p^2}{\epsilon_i^2} \right) \frac{1}{1 + (\omega_{c_i} \tau_i)^2} f_{0i} \tau_i, \quad (37)$$

$$\sigma_1 = \sum_i \frac{q_i^2 g_i}{3T} \int \frac{d^3 p}{(2\pi)^3} \left( \frac{p^2}{\epsilon_i^2} \right) \frac{\omega_{c_i} \tau_i}{1 + (\omega_{c_i} \tau_i)^2} f_{0i} \tau_i, \quad (38)$$

$$\sigma_2 = \sum_i \frac{q_i^2 g_i}{3T} \int \frac{d^3 p}{(2\pi)^3} \left( \frac{p^2}{\epsilon_i^2} \right) \frac{(\omega_{c_i} \tau_i)^2}{1 + (\omega_{c_i} \tau_i)^2} f_{0i} \tau_i. \quad (39)$$

Here  $\epsilon_i$ ,  $g_i$ ,  $\tau_i$  are the single particle dispersion relation, degeneracy factor, and relaxation time of ‘‘i’’th particle species. From Eq. (38), it is clear that Hall conductivity is zero at vanishing baryon chemical potential even at finite magnetic field. Only at finite baryon chemical potential Hall conductivity has nonvanishing value at finite magnetic field. Behavior of  $\sigma_0$  and  $\sigma_1$  with temperature, baryon chemical potential, and magnetic field has been discussed in Ref. [68]. In this investigation, we present variation of  $\sigma_2$  with temperature, baryon chemical potential, and magnetic field.

#### IV. SHEAR VISCOSITY IN THE PRESENCE OF MAGNETIC FIELD

Effect of magnetic field on shear viscosity of strongly interacting matter has been discussed in Refs. [74,76,98–101]. Without going into the details of the formalism, for completeness, we briefly mention here the salient features of the formalism. Following Refs. [74,76,98–101], we start with Boltzmann kinetic equation in the presence of magnetic field as discussed in Ref. [76],

$$p^\mu \partial_\mu f_0 + q B^{\mu\nu} \frac{\partial \delta f}{\partial u^\mu} u_\nu = C[\delta f]. \quad (40)$$

Here  $f_0$  is the equilibrium distribution function. In the Boltzmann approximation,  $f_0 = e^{-p^\mu U(x)_\mu / T \pm \mu_B / T}$ .  $U^\lambda \equiv (\gamma_V, \gamma_V \vec{V})$  is the macroscopic velocity of the fluid,  $p^\mu = m u^\mu$  is the particle four momentum,  $\delta f$  is the deviation from equilibrium, and  $B^{\mu\nu}$  is electromagnetic field tensor which contains magnetic field [76]. In Boltzmann approximation,

$$\partial_\mu f_0 = -\frac{f_0}{T} p^\lambda \partial_\mu U_\lambda(x). \quad (41)$$

In comoving frame, it can be shown that [76]

$$\partial_\mu f_0 |_{\vec{v}=0} = -\frac{f_0}{T} p_\nu \partial_\mu V^\nu. \quad (42)$$

Using Eq. (42), the Boltzmann equation (40) can be written as

$$-\frac{f_0}{T} p^\mu p^\nu V_{\mu\nu} = -q B^{\mu\nu} \frac{\partial \delta f}{\partial u^\mu} u_\nu + C[\delta f]. \quad (43)$$

Here  $V^{\mu\nu} = \frac{1}{2}(\partial^\mu V^\nu + \partial^\nu V^\mu)$ . Shear viscosity only deals with spatial variation of fluid velocity. Hence, we can drop all temporal dependence from the Boltzmann equation and only deal with spatial derivatives. Hence, the Boltzmann equation considering only the spatial derivatives of fluid velocity is

$$\frac{\epsilon}{T} p_\alpha v_\beta V_{\alpha\beta} f_0 = \frac{qB}{\epsilon} b_{\alpha\beta} v_\beta \frac{\partial(\delta f)}{\partial v^\alpha} + \frac{\delta f}{\tau}. \quad (44)$$

Here  $\alpha, \beta$  are spatial indices,  $b_{\alpha\beta} \equiv \epsilon_{\alpha\beta\gamma} b_\gamma$ ,  $b_\gamma = \frac{B_\gamma}{B}$ ,  $B^{\mu\nu}$  is the electromagnetic field tensor with  $\mu, \nu = \{0, 1, 2, 3\}$ .  $V_{\alpha\beta} = \frac{1}{2}(\partial_\alpha V_\beta + \partial_\beta V_\alpha)$ ,  $V_\alpha$  is the fluid velocity,  $p^\mu = (\epsilon, \vec{p})$  is the particle four momentum. Following Refs. [74,76], we can express  $\delta f$  in the following manner:

$$\delta f = \sum_{n=0}^{n=4} g_{(n)} V_{\alpha\beta}^{(n)} v_\alpha v_\beta, \quad (45)$$

where the tensors  $V_{\alpha\beta}^{(n)}$  are

$$\begin{aligned} V_{\alpha\beta}^{(0)} &= (3b_\alpha b_\beta - \delta_{\alpha\beta}) \left( b_\gamma b_\delta V_{\gamma\delta} - \frac{1}{3} \vec{\nabla} \cdot \vec{V} \right), \\ V_{\alpha\beta}^{(1)} &= 2V_{\alpha\beta} + \delta_{\alpha\beta} V_{\gamma\delta} b_\gamma b_\delta - 2V_{\alpha\gamma} b_\gamma b_\beta - 2V_{\beta\gamma} b_\gamma b_\alpha \\ &\quad + (b_\alpha b_\beta - \delta_{\alpha\beta}) \vec{\nabla} \cdot \vec{V} + b_\alpha b_\beta V_{\gamma\delta} b_\gamma b_\delta, \\ V_{\alpha\beta}^{(2)} &= 2(V_{\alpha\gamma} b_\beta b_\gamma + V_{\beta\gamma} b_\alpha b_\gamma - 2b_\alpha b_\beta V_{\gamma\delta} b_\gamma b_\delta), \\ V_{\alpha\beta}^{(3)} &= V_{\alpha\gamma} b_\beta b_\gamma + V_{\beta\gamma} b_\alpha b_\gamma - V_{\gamma\delta} b_{\alpha\gamma} b_\beta b_\delta - V_{\gamma\delta} b_{\beta\gamma} b_\alpha b_\delta, \\ V_{\alpha\beta}^{(4)} &= 2(V_{\gamma\delta} b_{\alpha\gamma} b_\beta b_\delta + V_{\gamma\delta} b_{\beta\gamma} b_\alpha b_\delta). \end{aligned} \quad (46)$$

Deviation of purely spatial components of the energy momentum tensor from equilibrium energy momentum tensor can be written as [76,98]

$$\delta T_{\alpha\beta} = \int \frac{d^3 p}{(2\pi)^3} v_\alpha v_\beta \epsilon \delta f. \quad (47)$$

Again using the functions  $V_{\alpha\beta}^{(n)}$ , we can write

$$\delta T_{\alpha\beta} = \sum_{n=0}^4 \eta_n V_{\alpha\beta}^{(n)}. \quad (48)$$

The viscosity component associated with the tensor  $V_{\alpha\beta}^{(0)}$  is the longitudinal viscosity as  $V_{\alpha\beta}^{(0)} b_\alpha b_\beta \neq 0$  while the components  $\eta^{(n)}$  corresponding to  $V_{\alpha\beta}^{(n)}$  ( $n = 1, 2, 3, 4$ ) are

$$\begin{aligned} \frac{\epsilon}{T} v_\alpha v_\beta V_{\alpha\beta} f_0 &= 2\omega_c g_1 [2V_{\alpha\gamma} b_{\alpha\beta} v_\beta v_\gamma - 2V_{\alpha\rho} b_{\alpha\beta} b_\rho v_\beta (\vec{b} \cdot \vec{v})] + 2\omega_c g_2 [2V_{\alpha\rho} b_{\alpha\beta} v_\beta b_\rho (\vec{v} \cdot \vec{b})] \\ &+ 2\omega_c g_3 [2V_{\alpha\beta} v_\alpha v_\beta - 4V_{\alpha\beta} v_\alpha b_\beta (\vec{b} \cdot \vec{v})] + 2\omega_c g_4 [2V_{\alpha\beta} v_\alpha b_\beta (\vec{b} \cdot \vec{v})] \\ &+ \frac{g_1}{\tau} [2V_{\gamma\delta} v_\gamma v_\delta - 4V_{\gamma\rho} v_\gamma b_\rho (\vec{b} \cdot \vec{v})] + \frac{g_2}{\tau} [4V_{\gamma\rho} v_\gamma b_\rho (\vec{b} \cdot \vec{v})] \\ &+ \frac{g_3}{\tau} [2V_{\gamma\rho} b_{\delta\rho} v_\gamma v_\delta - 2V_{\rho\sigma} b_{\gamma\rho} b_\sigma v_\gamma (\vec{b} \cdot \vec{v})] + \frac{g_4}{\tau} [4V_{\rho\sigma} b_{\gamma\rho} b_\sigma v_\gamma (\vec{b} \cdot \vec{v})]. \end{aligned} \quad (49)$$

To get Eq. (49), we have used  $\vec{\nabla} \cdot \vec{v} = 0$ ,  $V_{\alpha\beta} b_\alpha b_\beta = 0$ ,  $b_{\alpha\beta} b_\alpha = 0$ ,  $b_{\alpha\beta} v_\alpha v_\beta = 0$ , and  $b_\alpha b_\alpha = 1$ . Comparing various tensor structure in Eq. (49), we can write

$$\begin{aligned} g_3 &= 2\omega_c \tau g_1 \\ 2\omega_c g_3 - \omega_c g_4 + \frac{g_1}{\tau} - \frac{g_2}{\tau} &= 0 \\ 4\omega_c g_1 - 4\omega_c g_2 + \frac{2}{\tau} g_3 - \frac{4}{\tau} g_4 &= 0 \\ 2\omega_c g_3 + \frac{1}{\tau} g_1 &= \frac{\epsilon}{2T} f_0. \end{aligned} \quad (50)$$

Solving the above set of equations for the coefficients  $g_1$ ,  $g_2$ ,  $g_3$ , and  $g_4$ , we get

$$g_1 = \frac{\epsilon}{2T} \frac{\tau}{[1 + 4(\omega_c \tau)^2]} f_0, \quad (51)$$

$$g_2 = \frac{\epsilon}{2T} \frac{\tau}{[1 + (\omega_c \tau)^2]} f_0, \quad (52)$$

$$g_3 = \frac{\epsilon}{2T} \frac{\tau(\omega_c \tau)}{[\frac{1}{2} + 2(\omega_c \tau)^2]} f_0, \quad (53)$$

$$g_4 = \frac{\epsilon}{2T} \frac{\tau(\omega_c \tau)}{[1 + (\omega_c \tau)^2]} f_0. \quad (54)$$

Using Eqs. (47) and (48), various components of the shear viscosity in magnetic field can be shown to be [76,98]

$$\eta_n = \frac{2}{15} \int \frac{d^3 p}{(2\pi)^3} \epsilon g_n v^4, \quad n = 1, 2, 3, 4, \quad (55)$$

so that

called the transverse viscosities as they are transverse to  $b_\alpha b_\beta$ . To calculate transverse shear viscosity coefficients, we impose the conditions  $\vec{\nabla} \cdot \vec{v} = 0$  and  $V_{\gamma\delta} b_\gamma b_\delta = 0$  [74,76]. Hence,  $V_{\alpha\beta}^{(0)} = 0$ . Using the tensors  $V_{\alpha\beta}^{(n)}$ ,  $n = 1, 2, 3, 4$ , Eq. (44) can be expressed as (for details, see Refs. [76,98–100])

$$\eta_1 = \frac{1}{15T} \int \frac{d^3 p}{(2\pi)^3} \frac{p^4}{\epsilon^2} \frac{\tau}{1 + 4(\omega_c \tau)^2} f_0, \quad (56)$$

$$\eta_2 = \frac{1}{15T} \int \frac{d^3 p}{(2\pi)^3} \frac{p^4}{\epsilon^2} \frac{\tau}{1 + (\omega_c \tau)^2} f_0, \quad (57)$$

$$\eta_3 = \frac{1}{15T} \int \frac{d^3 p}{(2\pi)^3} \frac{p^4}{\epsilon^2} \frac{\tau(\omega_c \tau)}{\frac{1}{2} + 2(\omega_c \tau)^2} f_0, \quad (58)$$

$$\eta_4 = \frac{1}{15T} \int \frac{d^3 p}{(2\pi)^3} \frac{p^4}{\epsilon^2} \frac{\tau(\omega_c \tau)}{1 + (\omega_c \tau)^2} f_0. \quad (59)$$

For hadron resonance gas model, total shear viscosity in the presence of magnetic field can be expressed as

$$\eta_1 = \sum_i \frac{g_i}{15T} \int \frac{d^3 p}{(2\pi)^3} \frac{p^4}{\epsilon_i^2} \frac{1}{1 + 4(\omega_{c_i} \tau_i)^2} f_{0_i} \tau_i, \quad (60)$$

$$\eta_2 = \sum_i \frac{g_i}{15T} \int \frac{d^3 p}{(2\pi)^3} \frac{p^4}{\epsilon_i^2} \frac{1}{1 + (\omega_{c_i} \tau_i)^2} f_{0_i} \tau_i, \quad (61)$$

$$\eta_3 = \sum_i \frac{g_i}{15T} \int \frac{d^3 p}{(2\pi)^3} \frac{p^4}{\epsilon_i^2} \frac{(\omega_{c_i} \tau_i)}{\frac{1}{2} + 2(\omega_{c_i} \tau_i)^2} f_{0_i} \tau_i, \quad (62)$$

$$\eta_4 = \sum_i \frac{g_i}{15T} \int \frac{d^3 p}{(2\pi)^3} \frac{p^4}{\epsilon_i^2} \frac{(\omega_{c_i} \tau_i)}{1 + (\omega_{c_i} \tau_i)^2} f_{0_i} \tau_i. \quad (63)$$

In Eqs. (60)–(63),  $g_i$ ,  $\tau_i$  are degeneracy factor and relaxation time of “i”th hadron.  $g_i$  in Eqs. (60)–(63) should not be confused with  $g_1, g_2, g_3, g_4$  as given in Eqs. (51)–(54). In the absence of magnetic field, only  $V_{\alpha\beta}^{(1)}$  is nonvanishing and the corresponding shear viscosity is  $\eta_1$ . In the absence

of magnetic field,  $\eta_1 = \eta_2$  and  $\eta_3 = \eta_4 = 0$ .  $\eta_3$  and  $\eta_4$  are Hall-type shear viscosities. Similar to other Hall-type transport coefficients, Hall-type shear viscosity also vanishes for zero baryon chemical potential even for nonvanishing magnetic field. This is because, at vanishing baryon chemical potential, when the number density of particles and antiparticles are same, particles and antiparticles will have equal and opposite contribution to shear viscosity  $\eta_3$  and  $\eta_4$ . Only at finite baryon chemical potential,  $\eta_3$  and  $\eta_4$  can take nonvanishing values. In this context, a comment regarding the anisotropic  $\eta$  may be in order. First, let us note that  $\eta_i$  ( $i = 1, 2, 3, 4$ ) is smaller compared to the longitudinal viscosity coefficient  $\eta_0$ . Therefore, the flow velocity in the direction perpendicular to the direction of the magnetic field will be larger as compared to the case in the absence of magnetic field.

In Refs. [102,103], transport coefficients have been calculated using a 14-moment approximation for dissipative magnetohydrodynamics. In these studies, the effects of Landau quantization have not been considered. As is the case in the present work, the effect of Landau quantization is not included and further more number of transport coefficients arise in the presence of magnetic field. However, the viscous stress is decomposed in a different basis as compared to Refs. [102,103]. Therefore, the different components of the shear viscosity are not same as in Refs. [102,103]. However, one can relate these two basis as has been shown, e.g., in Ref. [101].

To make a comparison between 14-moment method of Refs. [102,103], one might compare the expression for different viscosity coefficients for the case of massless Boltzmann gas which has been given in Ref. [102]. To this end, we define  $\eta_0$ , the viscosity coefficient without magnetic field for massless Boltzmann gas in the relaxation time approximation, e.g., for a single species.

For the massless Boltzmann gas, it can be shown that

$$\eta_0 = \frac{g}{15T} \int \frac{d^3 p}{(2\pi)^3} \frac{p^4}{\epsilon^2} f_0 \tau = \frac{4\lambda_{\text{mfp}} P}{5}, \quad (64)$$

where the mean free path  $\lambda_{\text{mfp}} = v\tau \equiv \tau$  for massless particles and  $P$  denotes pressure which can be expressed as

$$P = g \int \frac{d^3 p}{(2\pi)^3} \frac{p^2}{3\epsilon} f_0. \quad (65)$$

This  $\eta_0$  differs by a factor  $3/5$  from 14-moment method estimation of  $\eta_{0(14)} = \frac{4}{3}\lambda_{\text{mfp}} P$ . Then the relationship between  $\eta_i$ 's as evaluated here and  $\eta_{ij}$ 's of 14-moment method is given as

$$\begin{aligned} \eta_{00(14)}(\xi_B) &= \frac{5}{3}\eta_1(\xi_B), \\ \eta_{02(14)}(\xi_B) &= \frac{5}{3}(\eta_2(\xi_B) - \eta_1(\xi_B)), \\ \eta_{03(14)}(\xi_B) &= \frac{5}{3}\eta_3(\xi_B)/2, \\ \eta_{04(14)}(\xi_B) &= \frac{5}{3}\eta_4(\xi_B), \end{aligned} \quad (66)$$

where  $\xi_B = \frac{qB\lambda_{\text{mfp}}}{T}$ . To derive this, we have replaced  $\omega_c \tau \equiv \frac{qB\tau}{\epsilon(P)}$  by its thermal averaged value, i.e.,  $\frac{qB\tau}{\bar{\epsilon}} \equiv \frac{1}{3}\xi_B$ , where  $\bar{\epsilon} = 3T$ , the average single particle energy at a given temperature. Here we have not compared  $\eta_{01(14)}(\xi_B)$  as it has been shown in Ref. [101] that  $\eta_{01(14)}(\xi_B)$  is related to the bulk viscosity in the magnetic field. However, in this investigation, we have not studied bulk viscosity tensor in the presence of magnetic field. In Refs. [102,103], authors have found the Hall-type shear viscosities ( $\eta_{03(14)}, \eta_{04(14)}$ ) which are independent of the mean free path ( $\lambda_{\text{mfp}}$ ), for a large ratio of the mean free path to thermal Larmor radius ( $\xi_B \gg 1$ ). This behavior of Hall-type viscosities is similar to present results.

From Eqs. (19)–(21), (37)–(39), and (60)–(63), it is clear that the important input required for the estimation of the transport coefficient is the relaxation time  $\tau^i$  which in general can be energy dependent. In this investigation, we consider only energy averaged relaxation time. Further, the coefficients of thermal conductivity are dependent on bulk thermodynamic properties of the system, e.g., energy density, pressure, and enthalpy. These thermodynamic quantities and the relaxation time will be estimated for the hadronic system within the hadron resonance gas model that we discuss in the next section.

## V. HADRON RESONANCE GAS MODEL

The thermodynamic potential of a noninteracting gas of hadrons and its resonances at finite temperature ( $T$ ) and baryon chemical potential ( $\mu_B$ ) can be expressed as [53]

$$\begin{aligned} \log Z(\beta, \mu_B, V) &= \int dm (\rho_M(m) \log Z_b(m, V, \beta, \mu_B) \\ &+ \rho_B(m) \log Z_f(m, V, \beta, \mu_B)), \end{aligned} \quad (67)$$

where  $V$  is the volume and  $T = 1/\beta$  is the temperature of pointlike hadrons and their resonances. Total partition function is sum of the partition functions of free mesons ( $Z_b$ ) and baryons ( $Z_f$ ) with mass  $m$ . Moreover, spectral function which encodes hadron properties are represented as  $\rho_B$  and  $\rho_M$  for free mesons and baryons, respectively. Various thermodynamic quantities can be calculated using derivatives of the logarithm of the partition function as given in Eq. (67), with respect to the thermodynamic

parameters  $T$ ,  $\mu_B$ , and the volume  $V$ . In this investigation, we confine ourselves to ideal HRG model where we have considered all the hadrons and their resonances below a certain mass cutoff  $\Lambda$ . This can be achieved by taking the following form of spectral density:

$$\rho_{B/M}(m) = \sum_i^{m_i < \Lambda} g_i \delta(m - m_i). \quad (68)$$

Here  $m_i$  and  $g_i$  are mass and degeneracy of “ith” hadron species. Although HRG with discrete particle spectrum is very appealing because of its simple structure, but it can explain lattice QCD data for trace anomaly only up to temperature  $\sim 130$  MeV [104]. Including Hagedorn spectrum along with discrete particle spectrum HRG model can explain lattice QCD data for QCD trace anomaly up to  $T \sim 160$  MeV [104]. For details of thermodynamics of HRG model, see, e.g., Ref. [82].

The relaxation time of particle  $a$  with three momentum  $p_a$  and energy  $\epsilon_a$  is expressed as [40,105]

$$\tau_a^{-1}(\epsilon_a) = \sum_{b,c,d} \int \frac{d^3 p_b}{(2\pi)^3} \frac{d^3 p_c}{(2\pi)^3} \frac{d^3 p_d}{(2\pi)^3} W(a, b \rightarrow c, d) f_b^0. \quad (69)$$

Here  $W(a, b \rightarrow c, d)$  is the transition rate for process  $a(p_a) + b(p_b) \rightarrow c(p_c) + d(p_d)$  and can be expressed in terms of the transition amplitude  $\mathcal{M}$  in the following way:

$$W(a, b \rightarrow c, d) = \frac{(2\pi)^4 \delta(p_a + p_b - p_c - p_d)}{2\epsilon_a 2\epsilon_b 2\epsilon_c 2\epsilon_d} |\mathcal{M}|^2. \quad (70)$$

In the center of mass (c.m.) frame, the relaxation time ( $\tau_a$ ) or equivalently interaction frequency ( $\omega_a$ ) can be written as

$$\tau_a^{-1}(\epsilon_a) \equiv \omega_a(\epsilon_a) = \sum_b \int \frac{d^3 p_b}{(2\pi)^3} \sigma_{ab} v_{ab} f_b^0. \quad (71)$$

Here  $\sigma_{ab}$  is the total scattering cross section for the process  $a(p_a) + b(p_b) \rightarrow c(p_c) + d(p_d)$  and  $v_{ab}$  is the relativistic relative velocity between particles  $a$  and  $b$ ,

$$v_{ab} = \frac{\sqrt{(p_a \cdot p_b)^2 - m_a^2 m_b^2}}{\epsilon_a \epsilon_b}. \quad (72)$$

In this work, we shall be considering energy averaged relaxation time. One can obtain the energy independent relaxation time  $\tau^a$  by averaging the relaxation time  $\tau^a(\epsilon_a)$  over the distribution function  $f_a^0(\epsilon_a)$  [40,97],

$$\tau_a^{-1} = \frac{\int \frac{d^3 p_a}{(2\pi)^3} f_a^0 \tau_a^{-1}(\epsilon_a)}{\int \frac{d^3 p_a}{(2\pi)^3} f_a^0} = \sum_b \frac{\int \frac{d^3 p_a}{(2\pi)^3} \frac{d^3 p_b}{(2\pi)^3} f_a^0 f_b^0 \sigma_{ab} v_{ab}}{\int \frac{d^3 p_a}{(2\pi)^3} f_a^0}. \quad (73)$$

Using Eq. (73), the energy averaged relaxation time ( $\tau_a$ ) can be expressed as [62]

$$\tau_a^{-1} = \sum_b n_b \langle \sigma_{ab} v_{ab} \rangle, \quad \text{where,} \quad n_b = \int \frac{d^3 p_b}{(2\pi)^3} f_b^0. \quad (74)$$

Here  $n_b$  and  $\langle \sigma_{ab} v_{ab} \rangle$  represent number density and thermal averaged cross section, respectively. The thermal averaged cross section for the scattering process  $a(p_a) + b(p_b) \rightarrow c(p_c) + d(p_d)$  is given as [106]

$$\langle \sigma_{ab} v_{ab} \rangle = \frac{\int d^3 p_a d^3 p_b \sigma_{ab} v_{ab} f_a^0(p_a) f_b^0(p_b)}{\int d^3 p_a d^3 p_b f_a^0(p_a) f_b^0(p_b)}. \quad (75)$$

In Boltzmann approximation and for hard sphere (of radius  $r_h$ ) scattering for the cross section ( $\sigma = 4\pi r_h^2$ ), the thermal averaged cross section becomes

$$\langle \sigma_{ab} v_{ab} \rangle = \frac{\sigma \int d^3 p_a d^3 p_b v_{ab} e^{-\epsilon_a/T} e^{-\epsilon_b/T}}{\int d^3 p_a d^3 p_b e^{-\epsilon_a/T} e^{-\epsilon_b/T}}. \quad (76)$$

Note that in Boltzmann approximation of the thermal averaged relaxation time chemical potential dependence gets canceled from the numerator and denominator. Rather than using momentum integration it is useful to introduced c.m. energy variable ( $\sqrt{s}$ ) to calculate thermal averaged cross section. In terms of c.m. energy variable ( $\sqrt{s}$ ), it can be shown that

$$\begin{aligned} & \int d^3 p_a d^3 p_b v_{ab} e^{-\epsilon_a/T} e^{-\epsilon_b/T} \\ &= 2\pi^2 T \int ds \sqrt{s} (s - 4m^2) K_1(\sqrt{s}/T) \end{aligned} \quad (77)$$

and

$$\int d^3 p_a d^3 p_b e^{-\epsilon_a/T} e^{-\epsilon_b/T} = (4\pi m^2 T K_2(m/T))^2. \quad (78)$$

Thus, the thermal averaged cross section can be given as

$$\langle \sigma_{ab} v_{ab} \rangle = \frac{\sigma}{8m^4 T K_2^2(m/T)} \int_{4m^2}^{\infty} ds \sqrt{s} (s - 4m^2) K_1(\sqrt{s}/T). \quad (79)$$

Here  $\sqrt{s}$  is the c.m. energy,  $K_1$  and  $K_2$  are modified Bessel function of first order and second order, respectively. When the particles are of different species, then the above equation can be generalized as

$$\begin{aligned}
\langle \sigma_{ab} v_{ab} \rangle &= \frac{\sigma}{8T m_a^2 m_b^2 K_2(m_a/T) K_2(m_b/T)} \\
&\times \int_{(m_a+m_b)^2}^{\infty} ds \times \frac{[s - (m_a - m_b)^2]}{\sqrt{s}} \\
&\times [s - (m_a + m_b)^2] K_1(\sqrt{s}/T), \quad (80)
\end{aligned}$$

where  $\sigma = 4\pi r_h^2$  is the total scattering cross section for the hard sphere. It is important to mention that in hard sphere scattering approximation section  $\sigma$  is independent of temperature and baryon chemical potential. But thermal averaged cross section  $\langle \sigma v \rangle$  in general can depend on temperature ( $T$ ) and chemical potential  $\mu_B$ . Only in Boltzmann approximation,  $\langle \sigma v \rangle$  is independent of  $\mu_B$  [106]. Evaluating the thermal averaged relaxation time for each species, we estimate various transport coefficients of the hot and dense hadron gas.

## VI. RESULTS AND DISCUSSIONS

We have estimated thermal conductivity, electrical conductivity, and shear viscosity in the presence of magnetic field within the framework of hadron resonance gas model. For the hadron resonance gas model, we consider all the hadrons and their resonances up to a mass cutoff  $\Lambda$  which we take as  $\Lambda = 2.6$  GeV as is listed in Ref. [107]. For a detailed list of hadrons and its resonances, we refer to Appendix A of Ref. [108]. Apart from these parameters radii of the hard spheres also enter in the calculation of relaxation time. We have considered a uniform radius of  $r_h = 0.5$  fm for all the hadrons [62,109]. With these set of parameters, we have estimated thermal conductivity, shear viscosity, etc. as a function of temperature ( $T$ ) and baryon chemical potential ( $\mu_B$ ) for different values of the magnetic field ( $B$ ).

### A. Results for thermal conductivities in a magnetic field

In Fig. 1, we show the variation of normalized thermal conductivity ( $k_0/T^2$ ) with temperature ( $T$ ) for various values of magnetic field at a finite baryon chemical potential. As may be observed from the figure, the normalized thermal conductivity  $k_0/T^2$  decreases with temperature. Let us note that  $k_0/T^2$  as given in Eq. (19) depends on the relaxation time  $\omega/n_B$  and distribution function. As temperature increases, the scattering rate increases as the number of particle increases. This leads to relaxation time, which is inverse of scattering rate, decreasing with temperature. Further  $\omega/n_B$  also decreases with temperature which has been shown in the left plot in Fig. 2. The reason for this behavior of  $\omega/n_B$  with temperature can be understood as follows. The dominant contribution to the sum over all hadrons arises from pions and protons which can be approximately given by

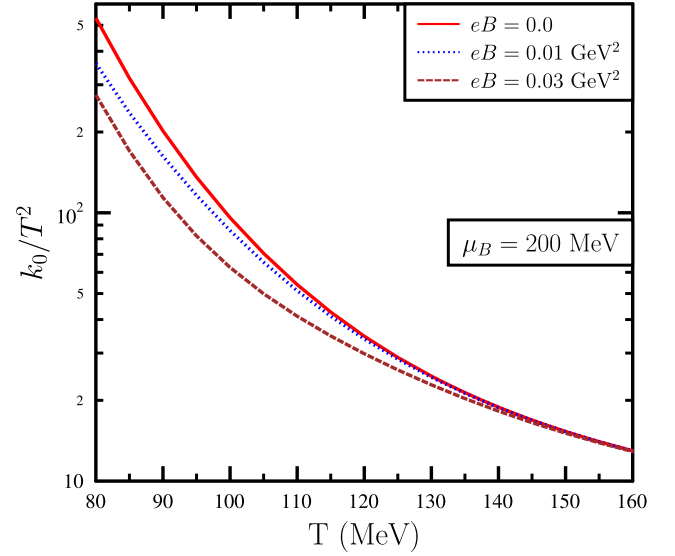


FIG. 1. Variation of normalized thermal conductivity ( $k_0/T^2$ ) with temperature ( $T$ ) for different values of magnetic field ( $B$ ) at finite baryon chemical potential. Red solid line represents  $B = 0$  case, blue dotted line and brown dashed line represent  $eB = 0.01$  GeV<sup>2</sup> and  $eB = 0.03$  GeV<sup>2</sup>, respectively. In the presence of magnetic field,  $k_0/T^2$  decreases. At low temperature, decrease in  $k_0/T^2$  due to magnetic field is significant. But at higher temperature, the effect of magnetic field on  $k_0/T^2$  is not significant.

$$\begin{aligned}
\frac{\omega}{n_B} &= \frac{\mathcal{E} + P}{n_B} \sim \frac{\mathcal{E}_\pi + P_\pi}{n_p} + \frac{\mathcal{E}_p + P_p}{n_p} \\
&\sim \frac{e^{-m_\pi/T}(m_\pi + T)}{\sinh(\mu_B/T)e^{-m_p/T}} + \frac{\cosh(\mu_B/T)e^{-m_p/T}(m_p + T)}{\sinh(\mu_B/T)e^{-m_p/T}}. \quad (81)
\end{aligned}$$

With increasing temperature,  $\coth(\mu_B/T)$  as well as  $(m_p + T)$  increases. Hence, if one considers only baryons, then with temperature  $\omega_B/n_B$  increases as can be seen in the right plot of Fig. 2. However, for pions,  $\omega_\pi/n_B$  decreases with temperature due to the term  $e^{(m_p - m_\pi)/T}$  in Eq. (81). For hadron resonance gas, contributions of mesons in the energy density and pressure are significantly large with respect to the baryonic contributions. Hence, when we consider hadron resonance gas, due to mesonic contribution to energy density and pressure,  $\omega/n_B$  decreases with temperature as can be seen in the left plot in Fig. 2.

It is also clear that in the presence of magnetic field thermal conductivity decreases. This can be understood from the expression for  $k_0/T^2$  in Eq. (19) which is inversely proportional to  $1 + (\omega_c \tau)^2$ . At low temperature, relaxation time is relatively larger and at low temperature  $k_0 \sim \frac{1}{\omega_c \tau}$ . Hence, at low temperature, magnetic field affects  $k_0/T^2$  significantly. On the other hand, at high temperature,  $\tau$  is small; hence, the effect of  $\omega_c \tau$  in the denominator of

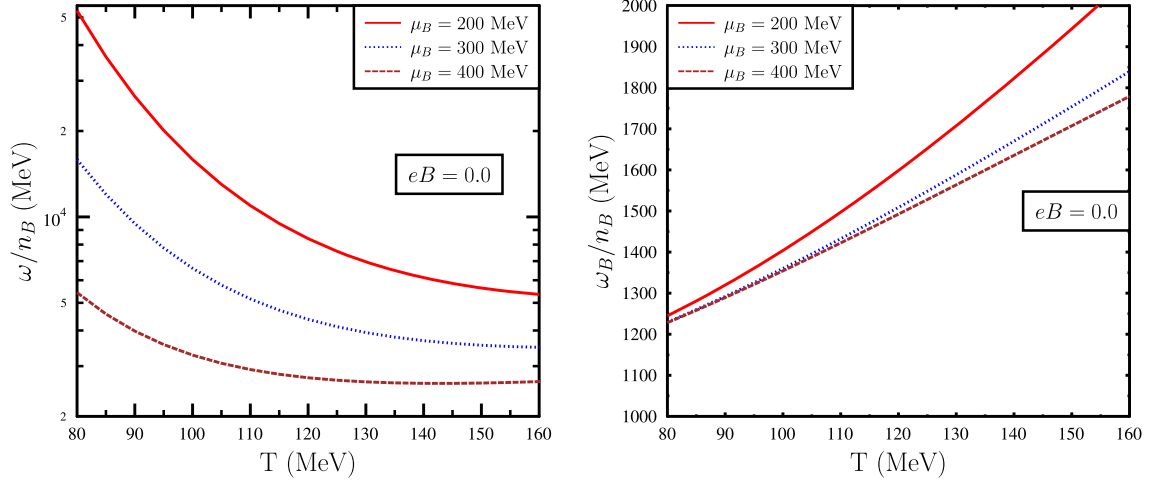


FIG. 2. Left plot: variation of  $\omega/n_B$  with temperature ( $T$ ) for different values of  $\mu_B$  at zero magnetic field. Right plot: variation of  $\omega/n_B$  only for baryons denoted as  $\omega_B/n_B$ , with temperature ( $T$ ) for different values of  $\mu_B$  for a vanishing magnetic field. With increasing temperature and  $\mu_B$ ,  $\omega/n_B$  of the hadron resonance gas decreases. However, baryonic contribution to  $\omega/n_B$  i.e.,  $\omega_B/n_B$  increases with temperature.

Eq. (19) is not significant. Thus, at small temperature,  $k_0/T^2$  decreases with magnetic field but at large temperature magnetic field does not affect  $k_0/T^2$  significantly. This behavior of thermal conductivity is analogous to the variation of electrical conductivity ( $\sigma_0/T$ ), as discussed in Ref. [68].

We next discuss the variation of  $k_0/T^2$  with  $\mu_B$  in Fig. 3. In the left panel, we show the result for vanishing magnetic field and for nonvanishing magnetic field on the right panel. With increasing  $\mu_B$  and temperature,  $k_0/T^2$  decreases. With increasing  $\mu_B$ , relaxation time of different hadrons and  $\omega/n_B$  decreases. Relaxation time decreases with  $\mu_B$ , due to the fact that with increasing  $\mu_B$  number density of the baryons increases. With increasing number density of the

baryons scattering rate increases. On the other hand, decreasing behavior of  $\omega/n_B$  with  $\mu_B$  can be understood using Eq. (81). From Eq. (81), it is clear that with increasing  $\mu_B$ , mesonic as well as baryonic contribution in  $\omega/n_B$  of hadron resonance gas decreases due to the factor  $\sinh(\mu_B/T)$  in the denominator. Mesonic contribution in energy density and pressure of hadron resonance gas is independent of  $\mu_B$ . On the other hand, number density of baryons ( $n_B$ ) increases with  $\mu_B$ . Thus, with increasing  $\mu_B$ , mesonic contribution in  $\omega/n_B$  decreases. Further, for baryons energy density, pressure and number density depend upon  $\mu_B$ . From Eq. (81), it is clear that energy density and pressure of baryons  $\sim \cosh(\mu_B/T)$ , but  $n_B \sim \sinh(\mu_B/T)$ . Hence, with increasing  $\mu_B$ , baryonic

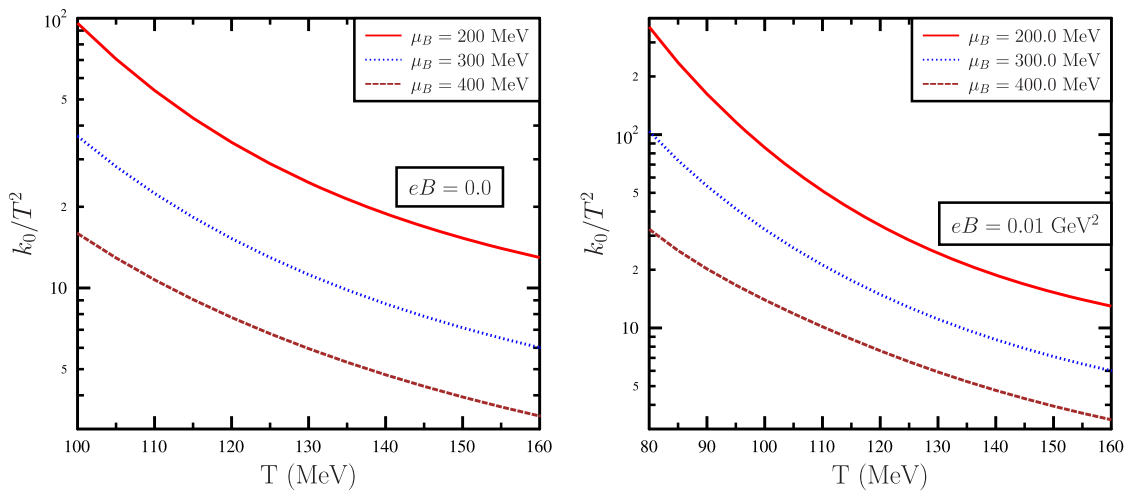


FIG. 3. Left plot: variation of normalized thermal conductivity ( $k_0/T^2$ ) with temperature ( $T$ ) for different values of  $\mu_B$  at zero magnetic field. Right plot: variation of normalized thermal conductivity ( $k_0/T^2$ ) with temperature ( $T$ ) for different values of  $\mu_B$  for a nonvanishing magnetic field. With increasing temperature and  $\mu_B$ ,  $k_0/T^2$  decreases. In the presence of magnetic field,  $k_0/T^2$  decreases.

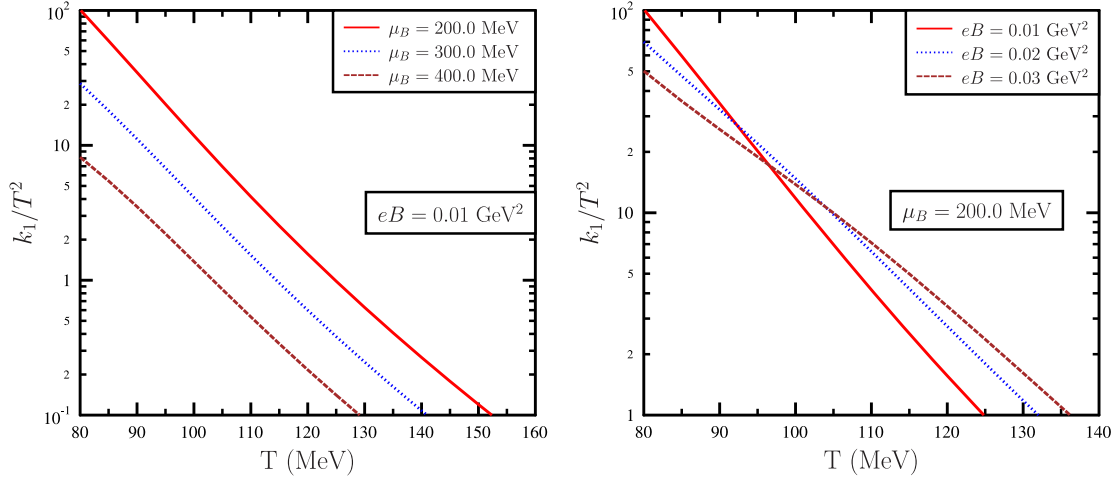


FIG. 4. Left plot: variation of Hall-type thermal conductivity  $k_1/T^2$  with temperature for nonvanishing magnetic field and different values of  $\mu_B$ . Right plot: variation of  $k_1/T^2$  with temperature for different values of magnetic fields. With  $\mu_B$   $k_1/T^2$  decreases. But for a fixed value of  $\mu_B$  variation of  $k_1/T^2$  is nonmonotonic with magnetic field. At low temperature,  $k_1/T^2$  decreases with magnetic field, but at higher temperature  $k_1/T^2$  increases with magnetic field.

contribution in  $\omega/n_B$  of the hadron resonance gas decreases. Decreasing behavior of  $\omega/n_B$  with  $\mu_B$  has been shown in Fig. 2. For the range of temperature and  $\mu_B$  considered in this investigation, decrease of  $\tau$  and  $\omega/n_B$  is dominant with respect to increasing  $f_0$  with  $\mu_B$ . Hence, with  $\mu_B$ ,  $k_0/T^2$  of the hot and dense hadron gas decreases. It may be noted that as  $\mu_B \rightarrow 0$ , thermal conductivity diverges as  $n_B^{-2}$ . This divergence is inconsequential as the factor  $k_0 n_B^2$  enters the equation of motion. Since  $k_0 n_B^2$  remains finite as  $\mu_B \rightarrow 0$ , transport due to thermal conduction becomes irrelevant as  $\vec{\nabla}(\mu_B/T) \rightarrow 0$  [4]. For  $\mu_B \rightarrow 0$ , relevant transport processes are only momentum diffusion through viscous stresses. Such behavior was also seen in Ref. [97]. For nonvanishing magnetic field,  $k_0/T^2$  decreases due to  $(\omega_c \tau)^2$  factor in the denominator of expression for  $k_0$ .

In Fig. 4, we show the variation of Hall-type thermal conductivity ( $k_1/T^2$ ) with temperature. For vanishing magnetic field,  $k_1/T^2$  is zero as can be seen from Eq. (20). Only at finite magnetic field and finite  $\mu_B$ ,  $k_1/T^2$  can have nonvanishing values. In the left plot in Fig. 4, we show the variation of  $k_1/T^2$  with temperature for nonvanishing values of  $\mu_B$  for a fixed value of magnetic field. It is clear from this plot that with  $\mu_B$ ,  $k_1/T^2$  decreases. This decrease is predominately due to a decrease of  $\omega/n_B$  factor with increasing  $\mu_B$ . On the other hand, for a fixed value of  $\mu_B$ ,  $k_1/T^2$  decreases with magnetic field at low temperature and increases with magnetic field at high temperature as can be seen in the right plot of Fig. 4. This behavior of  $k_1/T^2$  can be understood in the following way: at low temperature,  $\tau$  is large; hence, at low temperature  $k_1/T^2 \sim 1/\omega_c$ . On the other hand, at high temperature, relaxation time is small and  $k_1/T^2 \sim \omega_c$ . Thus,

variation of  $k_1/T^2$  is different with magnetic field at low temperature and high temperature.

In Fig. 5, variation of the third component of the thermal conductivity tensor  $k_2/T^2$  has been shown with temperature. It is clear for Eq. (21) that  $k_2/T^2$  has nonvanishing value only at finite magnetic field. In the right plot in Fig. 5, we show the variation of  $k_2/T^2$  with temperature at nonzero  $\mu_B$  for various values of magnetic field. In the left plot in Fig. 5, we show the variation of  $k_2/T^2$  with temperature and  $\mu_B$  for nonvanishing value of magnetic field. From the right plot in Fig. 5, we can see that with magnetic field  $k_2/T^2$  increases. However, for a large magnetic field and low temperature,  $k_2/T^2$  is not affected by magnetic field significantly. Naively this is because for low temperature the relaxation time is large; hence,  $\frac{(\omega_c \tau)^2}{1+(\omega_c \tau)^2} \sim 1$  for high magnetic fields. Similarly, at high temperature, when the relaxation time is small,  $k_2/T^2 \sim \tau^2 \omega_c^2$ . Hence, at high temperature, with increasing magnetic field  $k_2/T^2$  increases. In the left plot of Fig. 5, we show the variation of  $k_2/T^2$  for nonzero values of baryon chemical potential at finite magnetic field. In this plot, we can see that with  $\mu_B$ ,  $k_2/T^2$  decreases. Variation of  $k_2/T^2$  with  $\mu_B$  is convoluted because in the expression of  $k_2/T^2$  various terms are present which depend upon  $\mu_B$ , e.g., relaxation time, distribution function, etc. With increasing  $\mu_B$ , relaxation time as well as  $\omega/n_B$  decreases and  $f_0$  increases. But the increase of  $f_0$  with  $\mu_B$  is not large enough to compensate the decreasing behavior of  $\tau$  and  $\omega/n_B$ . Hence, with increasing  $\mu_B$ ,  $k_2/T^2$  decreases.

## B. Results for electrical conductivity in a magnetic field

In this subsection, we discuss the variation of electrical conductivity ( $\sigma_2/T$ ) with temperature, magnetic field, and

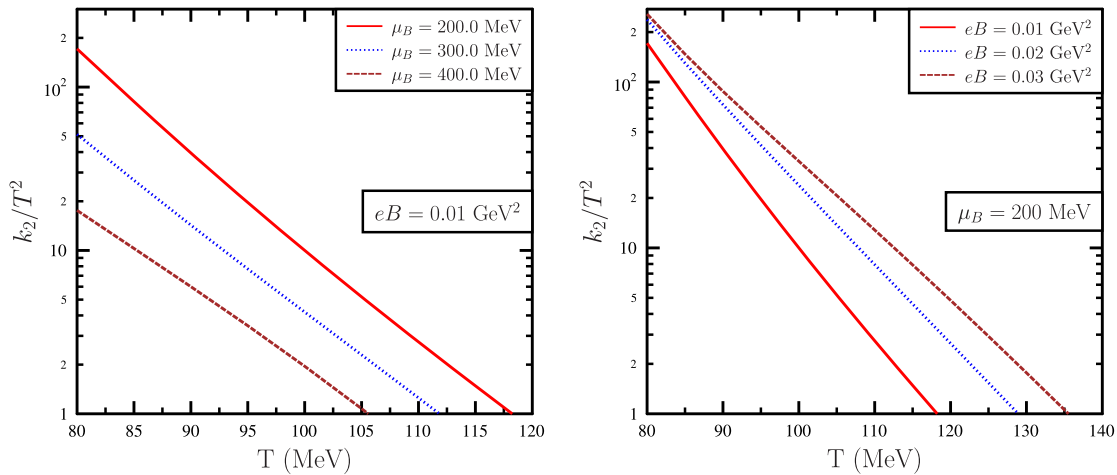


FIG. 5. Left plot: variation of  $k_2/T^2$  with temperature ( $T$ ) for various values of baryon chemical potential at finite magnetic field. Right plot: variation of  $k_2/T^2$  with temperature ( $T$ ) for various values of magnetic field. For a fixed value of magnetic field and  $\mu_B$ ,  $k_2/T^2$  decreases with temperature. With increasing magnetic field, generically  $k_2/T^2$  increases within the range of  $T$ ,  $\mu_B$ , and  $B$  considered in this investigation. But with increasing  $\mu_B$ ,  $k_2/T^2$  decreases.

baryon chemical potential. In our earlier work, we had demonstrated in details variation of  $\sigma_0$  and  $\sigma_1$  with temperature, magnetic field, and  $\mu_B$  [68]. Therefore, we do not repeat the discussion on the results for  $\sigma_0$  and  $\sigma_1$  here. Here we only show the variation of  $\sigma_2$  with temperature, baryon chemical potential, and magnetic field. In the left plot of Fig. 6, we show the variation of  $\sigma_2/T$  with temperature for a nonvanishing value of magnetic field but with different values of  $\mu_B$ . For a fixed value of magnetic field and  $\mu_B$ ,  $\sigma_2/T$  decreases with temperature. Among various hadrons, mesonic contribution to  $\sigma_2/T$  is large with respect to the baryonic contribution. With increasing temperature, mesonic contribution decreases due to decrease in the relaxation time of mesons. With increasing  $\mu_B$ , mesonic contribution to  $\sigma_2/T$  decreases and the baryonic

contribution increases. However, the decrease in mesonic contribution with increasing  $\mu_B$  is not compensated with increasing baryonic contribution for the range of temperature and baryon chemical potential considered here. Hence, with increasing  $\mu_B$ ,  $\sigma_2/T$  decreases. In the right plot in Fig. 6, we show the variation of  $\sigma_2/T$  with magnetic field. For the range of  $T$ ,  $\mu_B$ , and  $B$  we considered in this investigation,  $\sigma_2/T$  increases with magnetic field.

### C. Results for shear viscosity in a magnetic field

In Fig. 7, we show the variation of  $\eta_1/T^3$  with temperature for nonvanishing values of  $\mu_B$  for zero magnetic field. It is important to note that for zero magnetic field  $\eta_1 = \eta_2$  and  $\eta_3 = \eta_4 = 0$ . With temperature  $\eta_1/T^3$  decreases and it

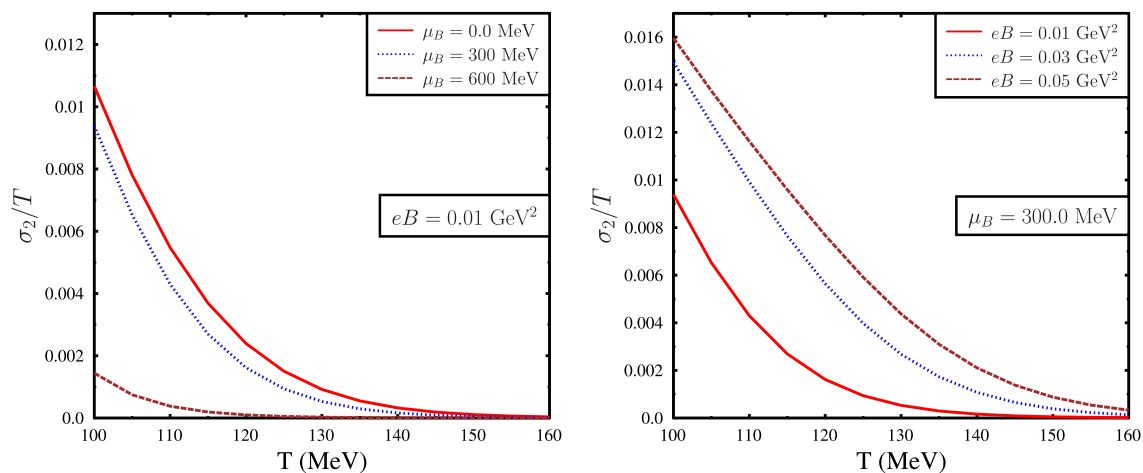


FIG. 6. Left plot: variation of  $\sigma_2/T$  with temperature for a nonvanishing magnetic field and for different values of  $\mu_B$ . With increasing  $\mu_B$ ,  $\sigma_2/T$  decreases. Right plot: variation of  $\sigma_2/T$  with temperature for nonvanishing values of magnetic field at finite  $\mu_B$ . With magnetic field,  $\sigma_2/T$  increases.

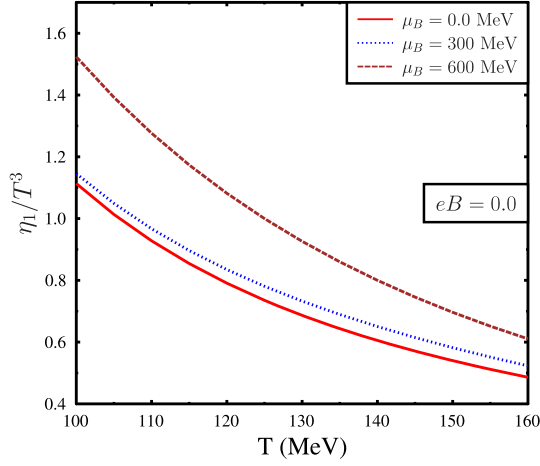


FIG. 7. Variation of  $\eta_1/T^3$  with temperature for vanishing magnetic field but with different values of  $\mu_B$ . At zero magnetic field,  $\eta_1 = \eta_2$ . From this figure, it is clear that  $\eta_1/T^3$  decreases with temperature and increases with  $\mu_B$ .

increases with  $\mu_B$ . This behavior of  $\eta_1/T^3$  with  $\mu_B$  is a combined effect of the variation of relaxation time and distribution function with  $\mu_B$ . Relaxation time decreases with  $\mu_B$ ; however, with increasing baryon, chemical potential  $f_0$  increases. Among various hadrons, mesonic contribution to  $\eta_1/T^3$  is larger as compared to the baryonic contribution at zero  $\mu_B$ . With increasing temperature, relaxation time of the hadrons decreases which gives rise to the decreasing behavior of  $\eta_1/T^3$  with temperature. On the other hand, with  $\mu_B$  mesonic contribution decreases due to a decrease in relaxation time with  $\mu_B$ ; however, with  $\mu_B$ , baryonic contribution increases due to the  $\mu_B$  factor in the distribution function. This increasing contributions of

baryons at finite  $\mu_B$  compensate decreasing contributions of the mesons. With increasing  $\mu_B$ , baryonic contribution becomes significant over mesonic contribution. Hence,  $\eta_1/T^3$  increases with  $\mu_B$  for a given  $T$  at vanishing magnetic field.

In Fig. 8, we show the variation of  $\eta_1/T^3$  and  $\eta_2/T^3$  with temperature for nonvanishing values of magnetic field at zero baryon chemical potential. From the expressions for  $\eta_1$  and  $\eta_2$ , it is clear that in the presence of magnetic field their behavior regarding variation with temperature is similar.  $\eta_1$  and  $\eta_2$  only differ in numerical values with  $\eta_1$  being little smaller as compared to  $\eta_2$  due to the different numerical factors in the denominator as given in Eqs. (56) and (57). From the left plot in Fig. 8, we can see that with magnetic field  $\eta_1/T^3$  decreases. This is due to  $(\omega_c \tau)^2$  factor in the denominator of Eq. (60). However, for a fixed value of magnetic field, variation of  $\eta_1/T^3$  with temperature is rather nonmonotonic in nature. The variation of  $\eta_1/T^3$  and  $\eta_2/T^3$  with temperature for a nonvanishing value of magnetic field shows a peak structure. These coefficients have three types of terms that depend upon temperature. The first one, the prefactor  $1/T^4$ , which always decreases with temperature, the  $\tau$  dependent factor  $\frac{\tau}{1+a(\omega_c \tau)^2}$  ( $a = 4$  for  $\eta_1$  and  $a = 1$  for  $\eta_2$ ), and the distribution function which always increases with temperature. At large temperature for which one can neglect  $a(\omega_c \tau)^2$  term due to small relaxation time compared to 1,  $\eta_1/T^3$  becomes linearly dependent on  $\tau$  and is independent of magnetic field. The decreasing behavior of the prefactor ( $1/T^4$ ) and  $\tau$  with temperature compensate for the increasing behavior of the distribution function resulting in a decreasing behavior of  $\eta_1/T^3$  reaching the zero-field limit. This explains the large temperature behavior of  $\eta_1/T^3$  and  $\eta_2/T^3$ , as seen in (8).

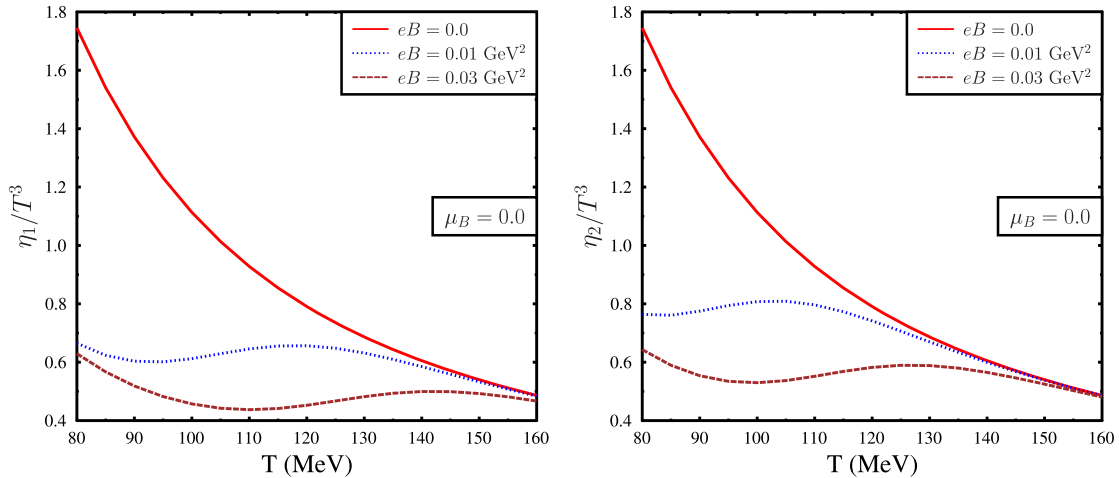


FIG. 8. Left plot: variation of  $\eta_1/T^3$  with temperature for vanishing  $\mu_B$  but with different values of magnetic field. Right plot: variation of  $\eta_2/T^3$  with temperature for vanishing  $\mu_B$  but with different values of magnetic field. For vanishing magnetic field,  $\eta_1 = \eta_2$ , which can be seen in this figure. Also, for nonvanishing magnetic field,  $\eta_1 \neq \eta_2$  can be seen in these plots. With increasing magnetic field, both  $\eta_1/T^3$  and  $\eta_2/T^3$  decrease. This decrease is very prominent at low temperature. At high temperature, the effect of magnetic field is not significant.

At a small temperature for which, the relaxation time is large enough so that  $\frac{\tau}{1+a(\omega_c\tau)^2} \sim \frac{1}{\omega_c^2\tau}$ , which is an increasing function of temperature as  $\tau$  decreases with temperature. However, the increasing behavior of  $\frac{1}{\omega_c^2\tau}$  and the distribution function are overshadowed by the decreasing behavior of the prefactor  $1/T^4$ , leading to an initial decreasing behavior of  $\eta_1/T^3$  and  $\eta_2/T^3$  at relatively low temperatures. As temperature increases further, the increasing behavior of  $\frac{1}{\omega_c^2\tau}$  and the distribution function become increasingly important and  $\eta_1/T^3$  and  $\eta_2/T^3$  start increasing. Finally, at a much larger temperature, where  $\omega_c\tau$  can be negligible,  $\eta_1/T^3$  and  $\eta_2/T^3$  approach the zero-field behavior of decreasing nature with temperature as mentioned earlier. This essentially explains the nonmonotonic behavior of  $\eta_1/T^3$  and  $\eta_2/T^3$  with temperature.

It is also important to note that at high temperature magnetic field does not affect  $\eta_1/T^3$  significantly. This is because at high temperature relaxation time is small; hence, the factor  $\omega_c\tau$  in the denominator of Eq. (60) is rather small. Hence, at high temperature, suppression effect due to magnetic field is not significant. In the right plot of Fig. 8, we show the variation of  $\eta_2/T$  with temperature for nonvanishing values of magnetic field at zero  $\mu_B$ . Behavior of  $\eta_2/T$  can also be understood in the same manner as we have discussed for  $\eta_1/T^3$ .

Next, we show the variation of  $\eta_1/T^3$  and  $\eta_2/T^3$  with temperature for a nonvanishing magnetic field and various values of  $\mu_B$  in Fig. 9. In the presence of magnetic field,  $\eta_1$  is smaller than  $\eta_2$  as can be seen from Eqs. (60) and (61). Besides this, variations of  $\eta_1/T^3$  and  $\eta_2/T^3$  are similar with temperature, magnetic field, and  $\mu_B$ . From Fig. 9, it is clear that variation of  $\eta_1/T^3$  and  $\eta_2/T^3$  with  $\mu_B$  is similar to Fig. 7, i.e., with  $\mu_B$ ,  $\eta_1/T^3$  and  $\eta_2/T^3$  increase. Mesonic

contribution to  $\eta_1/T^3$  and  $\eta_2/T^3$  is significantly larger than the baryonic contribution at vanishing  $\mu_B$ . With increasing  $\mu_B$ , mesonic contribution decreases due to a decrease in the relaxation time of mesons. On the other hand, with increasing  $\mu_B$ , baryonic contribution increases due to  $\mu_B$  factor in the distribution function. Increasing baryonic contribution compensates decreasing mesonic contribution to  $\eta_1/T^3$  and  $\eta_2/T^3$ . Hence, with increasing  $\mu_B$ , both  $\eta_1/T^3$  and  $\eta_2/T^3$  increase. However, in the presence of magnetic field, values of  $\eta_1$  and  $\eta_2$  are smaller with respect to the same in the absence of magnetic field. For a nonvanishing value of  $\mu_B$ , magnetic field variation of  $\eta_1/T^3$  and  $\eta_2/T^3$  with temperature is nonmonotonic and is similar to Fig. 8.

In Fig. 10, we show the variation of  $\eta_3/T^3$  and  $\eta_4/T^3$  with temperature for  $eB = 0.01 \text{ GeV}^2$  for values of  $\mu_B = 300 \text{ MeV}$  and  $\mu_B = 600 \text{ MeV}$ . Note that  $\eta_3$  and  $\eta_4$  are Hall-type shear viscosities in magnetic field. Hence,  $\eta_3$  and  $\eta_4$  are zero for zero magnetic field as well as for zero baryon chemical potential due to equal and opposite contributions of particles and antiparticles. Only at nonvanishing magnetic field and finite  $\mu_B$ ,  $\eta_3$  and  $\eta_4$  have nonvanishing values. From Fig. 10, we see that with  $\mu_B$  both  $\eta_3/T^3$  and  $\eta_4/T^3$  increase for nonvanishing value of magnetic field. This behavior of  $\eta_3$  and  $\eta_4$  can be understood naively in the following way. Due to Hall-type nature of  $\eta_3$  and  $\eta_4$ , only baryons contribute to  $\eta_3$  and  $\eta_4$  at finite  $\mu_B$ . With increasing  $\mu_B$ , the number density of baryons increases; this gives rise to increasing behavior of  $\eta_3/T^3$  and  $\eta_4/T^3$ .

In Fig. 11, we show the variation of  $\eta_3/T^3$  and  $\eta_4/T^3$  with temperature for  $\mu_B = 300 \text{ MeV}$  for different values of magnetic field. From this figure, we can see that with increasing magnetic field both  $\eta_3/T^3$  and  $\eta_4/T^3$  increase at large temperature. But at low temperature, both  $\eta_3/T^3$  and  $\eta_4/T^3$  decrease with magnetic field. This behavior of  $\eta_3/T^3$  and

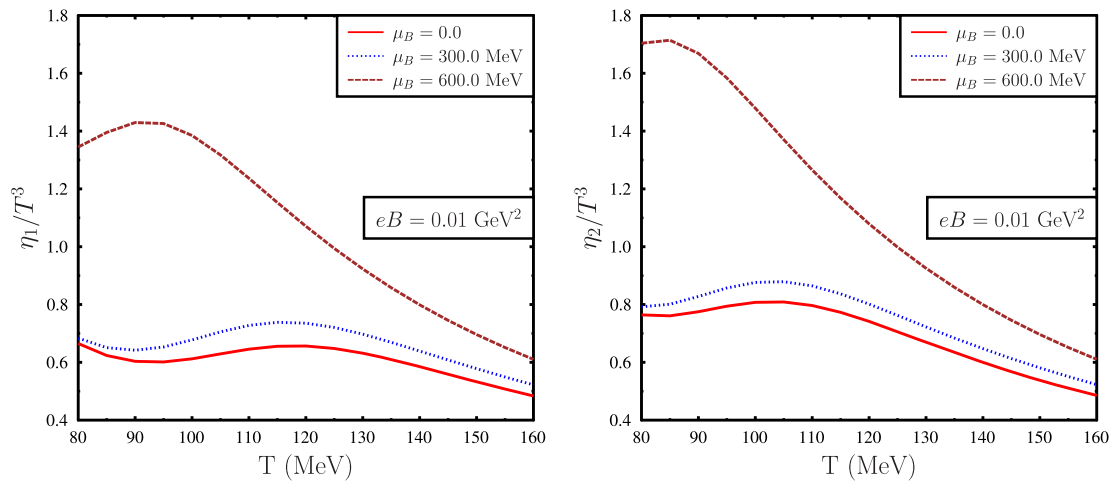


FIG. 9. Left plot: variation of  $\eta_1/T^3$  with temperature for different values of  $\mu_B$  in the presence of magnetic field. Right plot: variation of  $\eta_2/T^3$  with temperature for different values of  $\mu_B$  in the presence of magnetic field. Behavior of  $\eta_1/T^3$  and  $\eta_2/T^3$  is similar apart from their numerical values.  $\eta_2$  is larger than  $\eta_1$  as can be seen from their analytical expressions. For higher  $\mu_B$ , value of  $\eta_1/T^3$  and  $\eta_2/T^3$  is higher. Variation of both  $\eta_1/T^3$  and  $\eta_2/T^3$  with temperature shows nonmonotonic behavior with a peak structure.

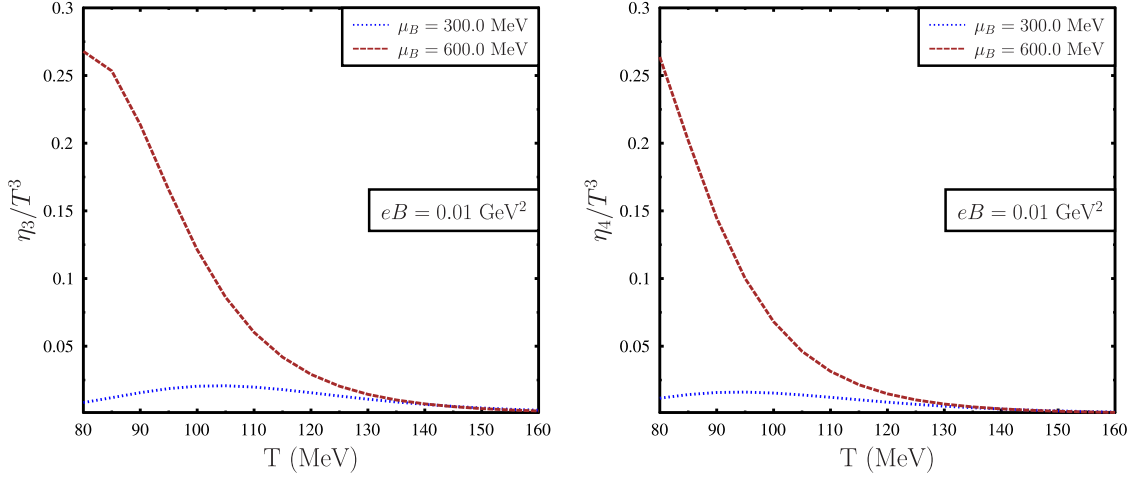


FIG. 10. Left plot: variation of  $\eta_3/T^3$  with temperature for a nonvanishing magnetic field and different values of  $\mu_B$ . Right plot: variation of  $\eta_4/T^3$  with temperature for a nonvanishing magnetic field and different values of  $\mu_B$ . Behavior of  $\eta_3/T^3$  and  $\eta_4/T^3$  is similar with  $\mu_B$  and temperature apart from their numerical values. With increasing  $\mu_B$ , Hall-type shear viscosities  $\eta_3/T^3$  and  $\eta_4/T^3$  increase.

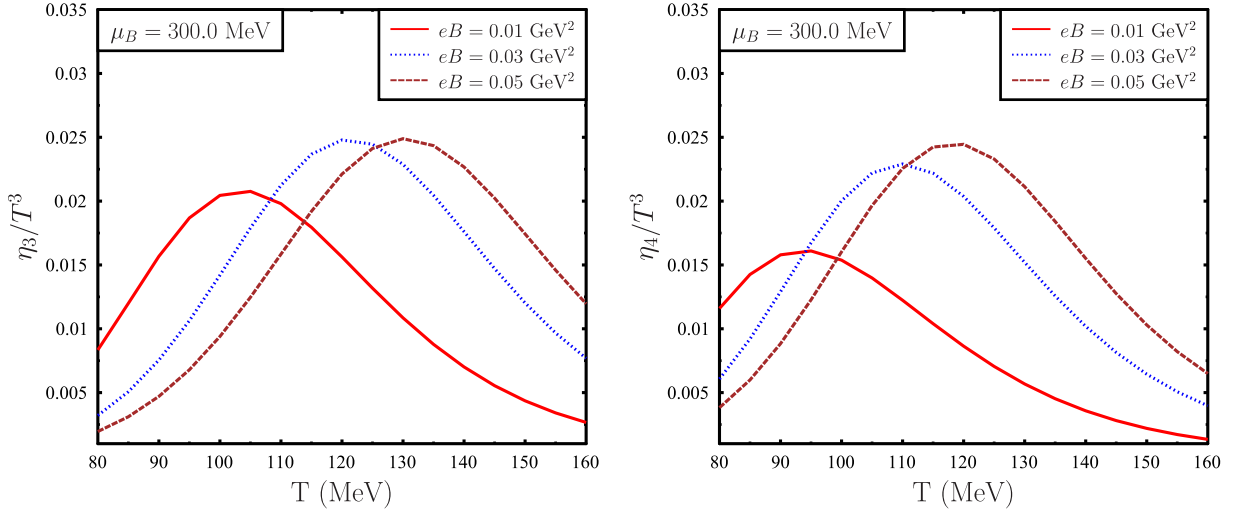


FIG. 11. Left plot: variation of  $\eta_3/T^3$  with temperature for different values of nonvanishing magnetic field and finite  $\mu_B$ . Right plot: variation of  $\eta_4/T^3$  with temperature for different values of nonvanishing magnetic field and finite  $\mu_B$ . Variation of  $\eta_3/T^3$  and  $\eta_4/T^3$  with temperature and magnetic field is similar apart from their numerical values. For low temperature,  $\eta_3/T^3$  and  $\eta_4/T^3$  decrease with magnetic field. On the other hand, for high temperature, both  $\eta_3/T^3$  and  $\eta_4/T^3$  increase with magnetic field. Variation of  $\eta_3/T^3$  and  $\eta_4/T^3$  with temperature is nonmonotonic with a peak.

$\eta_4/T^3$  is similar to the other Hall-type conductivities as discussed earlier. At low temperature, due to large value of relaxation time, both  $\eta_3/T^3$  and  $\eta_4/T^3 \sim 1/\omega_c$ . On the other hand, at high temperature, due to large relaxation time  $\eta_3/T^3 \sim \omega_c$ . This different behavior of  $\eta_3/T^3$  as well as  $\eta_4/T^3$  with magnetic field at high and low temperatures gives rise to nonmonotonic variation of these Hall-type shear viscosities with magnetic field.

Next, let us discuss temperature dependence of normalized Hall-type shear viscosities  $\eta_3/T^3$  and  $\eta_4/T^3$ . At large temperature, as may be observed from Eqs. (58) and (59),

both  $\eta_3/T^3$  and  $\eta_4/T^3 \sim \frac{1}{T^4} \tau^2 \omega_c$  vanish. This is because  $\omega_c$ , being inversely proportional to baryon mass, is small, as well as  $\tau$  itself, becomes vanishingly small at large temperatures. On the other hand, at small temperatures, with the relaxation time becoming larger, so  $1 + (\omega_c \tau)^2 \sim (\omega_c \tau)^2$  and  $\eta_3/T^3, \eta_4/T^3 \sim \frac{1}{T^4} \frac{1}{\omega_c} e^{-m_B/T}$ ,  $m_B$  being the baryon mass, which increases with temperature. Therefore, for some intermediate values between these two limits, one will have a maximum for  $\eta_3/T^3$  and  $\eta_4/T^3$ . Indeed, with increasing magnetic field, the peak occurs at higher temperatures, as may be clearly observed from Eq. (11).

It is also important to mention that the nonmonotonic behavior of shear viscosities is intimately related to the order of magnitude estimate of the relaxation time which is model dependent. If the relaxation time is very small, such that  $\omega_c \tau \ll 1$ , the variation of normalized shear viscosities will be linearly dependent on  $\tau$  (for  $\eta_1, \eta_2$ ). In this case, the behavior can be monotonically decreasing function of  $T$  as  $\tau$  decreases with  $T$ . This kind of situation can arise in various quasiparticle models of quark-gluon plasma, e.g., in Ref. [69] Hall conductivity has been studied for two different quasiparticle models of quark-gluon plasma. The variation of Hall conductivity is different in different quasiparticle models, as discussed in Ref. [69]. However, we expect that while this feature of nonmonotonic behavior will be there for hadronic models, in general, this may not hold good for quark matter described, e.g., by different quasiparticle models where the relaxation time can differ by an order of magnitude.

## VII. CONCLUSION

Off central heavy ion collisions can produce a strong magnetic field. The lifetime of such a field during the evolution of QGP to hadron gas depends critically on transport coefficients like electrical conductivity. Similarly, the other dissipative coefficients in the presence of magnetic field are also important and essential ingredients for the magnetohydrodynamic evolution of the strongly interacting medium produced subsequent to the collision. We have here attempted to evaluate some of these coefficients for magnetized hot and dense hadronic matter. The explicit calculations are performed within the hadron resonance gas model.

We have used the Boltzmann transport equation in the relaxation time approximation to estimate the transport coefficients. We have incorporated the effect of magnetic field through the cyclotron frequency of individual hadrons. Due to the vector nature of the field, the transport coefficients are no longer isotropic. It is observed that the anisotropic transport coefficients are always smaller than their isotropic counterpart at vanishing magnetic field. For strong fields, the effects arising from collision become

smaller compared to the effects arising from the cyclotron frequency.

For shear viscosity due to the presence of magnetic field, the transverse viscosity coefficient will be smaller compared to the longitudinal viscosity coefficient and will affect transverse flow. The structure of the viscous stress tensor in a magnetic field is model independent. However, the precise value of the transverse shear viscosity depends on the model considered. The viscous properties of the fluid extracted from flow data can lead to a more ideal fluid behavior in the presence of magnetic field as compared to the case in the absence of magnetic field [76].

In the context of electrical conductivity, it was shown that Hall conductivity  $\sigma_1$  for hadron gas generically increases with magnetic field [68]. It is also observed here that the non-Hall-type conductivity  $\sigma_2$  increases with magnetic field, while the component  $\sigma_0$  decreases with magnetic field. It is to be noted that  $\sigma = \sigma_0 + \sigma_2$  is the electrical conductivity in the absence of magnetic field.

Similar behavior is also observed for the anisotropic thermal conductivities ( $k_0, k_1$ , and  $k_2$ ). The ‘‘Hall-type’’ thermal conductivity  $k_1$  generically increases with magnetic field. The non-Hall-type conductivity  $k_0$  decreases with magnetic field, while  $k_2$  increases with magnetic field keeping  $k = k_0 + k_2$ , being independent of magnetic field with a value as one would obtain in the absence of magnetic field. In the present work, we have included the effect of magnetic field through cyclotron frequency of individual hadrons and have not taken the quantum effects arising from Landau quantization. Further, the relaxation time has been included with a hard sphere scattering where the effect of magnetic field is not included. Some of these calculations are in progress and will be reported elsewhere.

## ACKNOWLEDGMENTS

R.K.M. would like to thank PRL for support and local hospitality for her visit, during which this problem was initiated. R.K.M. would like to thank Basanta K. Nandi and Sadhana Dash for constant support and encouragement.

- 
- [1] U. W. Heinz and R. Snellings, *Annu. Rev. Nucl. Part. Sci.* **63**, 123 (2013).
  - [2] P. Romatschke and U. Romatschke, *Phys. Rev. Lett.* **99**, 172301 (2007).
  - [3] P. K. Kovtun, D. T. Son, and A. O. Starinets, *Phys. Rev. Lett.* **94**, 111601 (2005).
  - [4] S. Gavin, *Nucl. Phys.* **A435**, 826 (1985).
  - [5] A. Hosoya and K. Kajantie, *Nucl. Phys.* **B250**, 666 (1985).
  - [6] A. Dobado and J. M. Torres-Rincon, *Phys. Rev. D* **86**, 074021 (2012).
  - [7] C. Sasaki and K. Redlich, *Phys. Rev. C* **79**, 055207 (2009).
  - [8] C. Sasaki and K. Redlich, *Nucl. Phys.* **A832**, 62 (2010).
  - [9] F. Karsch, D. Kharzeev, and K. Tuchin, *Phys. Lett. B* **663**, 217 (2008).
  - [10] S. I. Finazzo, R. Rougemont, H. Marrochio, and J. Noronha, *J. High Energy Phys.* **02** (2015) 051.

- [11] A. Wiranata and M. Prakash, *Nucl. Phys.* **A830**, 219C (2009).
- [12] S. Jeon and L. Yaffe, *Phys. Rev. D* **53**, 5799 (1996).
- [13] D. E. Kharzeev, L. D. McLerran, and H. J. Warringa, *Nucl. Phys.* **A803**, 227 (2008).
- [14] V. Skokov, A. Y. Illarionov, and V. Toneev, *Int. J. Mod. Phys. A* **24**, 5925 (2009).
- [15] *Strongly Interacting Matter in Magnetic Field*, edited by D. Kharzeev, K. Landsteiner, A. Schmitt, and H. Yee, Lecture Notes in Physics Vol 871 (Springer-Verlag, Berlin, Heidelberg, 2013).
- [16] G. Inghirami, L. Del Zanna, A. Beraudo, M. H. Moghaddam, F. Becattini, and M. Bleicher, *Eur. Phys. J. C* **76**, 659 (2016).
- [17] A. Das, S. S. Dave, P. S. Saumia, and A. M. Srivastava, *Phys. Rev. C* **96**, 034902 (2017).
- [18] K. Tuchin, *Phys. Rev. C* **83**, 017901 (2011); **82**, 034904 (2010).
- [19] M. Greif, C. Greiner, and G. S. Denicol, *Phys. Rev. D* **93**, 096012 (2016).
- [20] M. Greif, I. Bouras, C. Greiner, and Z. Xu, *Phys. Rev. D* **90**, 094014 (2014).
- [21] A. Puglisi, S. Plumari, and V. Greco, *Phys. Lett. B* **751**, 326 (2015).
- [22] A. Puglisi, S. Plumari, and V. Greco, *Phys. Rev. D* **90**, 114009 (2014).
- [23] W. Cassing, O. Linnyk, T. Steinert, and V. Ozvenchuk, *Phys. Rev. Lett.* **110**, 182301 (2013).
- [24] T. Steinert and W. Cassing, *Phys. Rev. C* **89**, 035203 (2014).
- [25] G. Aarts, C. Allton, A. Amato, P. Giudice, S. Hands, and J.-I. Skullerud, *J. High Energy Phys.* **02** (2015) 186.
- [26] G. Aarts, C. Allton, J. Foley, S. Hands, and S. Kim, *Phys. Rev. Lett.* **99**, 022002 (2007).
- [27] A. Amato, G. Aarts, C. Allton, P. Giudice, S. Hands, and J.-I. Skullerud, *Phys. Rev. Lett.* **111**, 172001 (2013).
- [28] S. Gupta, *Phys. Lett. B* **597**, 57 (2004).
- [29] Y. Burnier and M. Laine, *Eur. Phys. J. C* **72**, 1902 (2012).
- [30] H.-T. Ding, A. Francis, O. Kaczmarek, F. Karsch, E. Laermann, and W. Soeldner, *Phys. Rev. D* **83**, 034504 (2011).
- [31] O. Kaczmarek and M. Muller, *Proc. Sci., LATTICE2013* (2014) 175.
- [32] S.-X. Qin, *Phys. Lett. B* **742**, 358 (2015).
- [33] R. Marty, E. Bratkovskaya, W. Cassing, J. Aichelin, and H. Berrehrah, *Phys. Rev. C* **88**, 045204 (2013).
- [34] D. Fernández-Fraile and A. Gomez Nicola, *Phys. Rev. D* **73**, 045025 (2006).
- [35] G. S. Denicol, H. Niemi, I. Bouras, E. Molnar, Z. Xu, D. H. Rischke, and C. Greiner, *Phys. Rev. D* **89**, 074005 (2014).
- [36] J. I. Kapusta and J. M. Torres-Rincon, *Phys. Rev. C* **86**, 054911 (2012).
- [37] M. Greif, J. A. Fotakis, G. S. Denicol, and C. Greiner, *Phys. Rev. Lett.* **120**, 242301 (2018).
- [38] M. Prakash, M. Prakash, R. Venugopalan, and G. Welke, *Phys. Rep.* **227**, 321 (1993).
- [39] A. Wiranata and Madappa Prakash, *Phys. Rev. C* **85**, 054908 (2012).
- [40] P. Chakraborty and J. I. Kapusta, *Phys. Rev. C* **83**, 014906 (2011).
- [41] A. S. Khvorostukhin, V. D. Toneev, and D. N. Voskresensky, *Nucl. Phys.* **A845**, 106 (2010).
- [42] S. Plumari, A. Paglisi, F. Scardina, and V. Greco, *Phys. Rev. C* **86**, 054902 (2012).
- [43] M. I. Gorenstein, M. Hauer, and O. N. Moroz, *Phys. Rev. C* **77**, 024911 (2008).
- [44] J. Noronha-Hostler, J. Noronha, and C. Greiner, *Phys. Rev. C* **86**, 024913 (2012).
- [45] S. K. Tiwari, P. K. Srivastava, and C. P. Singh, *Phys. Rev. C* **85**, 014908 (2012).
- [46] S. Ghosh, A. Lahiri, S. Majumder, R. Ray, and S. K. Ghosh, *Phys. Rev. C* **88**, 068201 (2013).
- [47] R. Lang, N. Kaiser, and W. Weise, *Eur. Phys. J. A* **51**, 127 (2015).
- [48] S. Ghosh, G. Krein, and S. Sarkar, *Phys. Rev. C* **89**, 045201 (2014).
- [49] A. Wiranata, V. Koch, M. Prakash, and X. N. Wang, *J. Phys. Conf. Ser.* **509**, 012049 (2014).
- [50] A. Wiranata, M. Prakash, and P. Chakraborty, *Central Eur. J. Phys.* **10**, 1349 (2012).
- [51] A. Tawfik and M. Wahba, *Ann. Phys. (Amsterdam)* **522**, 849 (2010).
- [52] J. Noronha-Hostler, J. Noronha, and C. Greiner, *Phys. Rev. Lett.* **103**, 172302 (2009).
- [53] G. Kadam and H. Mishra, *Nucl. Phys.* **A934**, 133 (2015).
- [54] G. Kadam, *Mod. Phys. Lett. A* **30**, 1550031 (2015).
- [55] S. Ghosh, *Int. J. Mod. Phys. A* **29**, 1450054 (2014).
- [56] N. Demir and A. Wiranata, *J. Phys. Conf. Ser.* **535**, 012018 (2014).
- [57] S. Ghosh, *Phys. Rev. C* **90**, 025202 (2014).
- [58] J.-B. Rose, J. M. Torres-Rincon, A. Schfer, D. R. Oliinychenko, and H. Petersen, *Phys. Rev. C* **97**, 055204 (2018).
- [59] C. Wesp, A. El, F. Reining, Z. Xu, I. Bouras, and C. Greiner, *Phys. Rev. C* **84**, 054911 (2011).
- [60] Moritz Greif, Ioannis Bouras, Carsten Greiner, and Zhe Xu, *Phys. Rev. D* **90**, 094014 (2014).
- [61] S. A. Bass *et al.*, *Prog. Part. Nucl. Phys.* **41**, 255 (1998).
- [62] G. Kadam and H. Mishra, *Phys. Rev. C* **92**, 035203 (2015).
- [63] R. K. Mohapatra, H. Mishra, S. Dash, and B. K. Nandi, [arXiv:1901.07238](https://arxiv.org/abs/1901.07238).
- [64] P. Singha, A. Abhishek, G. Kadam, S. Ghosh, and H. Mishra, *J. Phys. G* **46**, 015201 (2019).
- [65] A. Abhishek, H. Mishra, and S. Ghosh, *Phys. Rev. D* **97**, 014005 (2018).
- [66] J. R. Bhatt, A. Das, and H. Mishra, *Phys. Rev. D* **99**, 014015 (2019).
- [67] X. Huang, A. Sedrakian, and D. H. Rischke, *Ann. Phys. (Amsterdam)* **326**, 3075 (2011).
- [68] A. Das, H. Mishra, and R. K. Mohapatra, *Phys. Rev. D* **99**, 094031 (2019).
- [69] A. Das, H. Mishra, and R. K. Mohapatra, [arXiv:1907.05298](https://arxiv.org/abs/1907.05298).
- [70] C. Hamaguchi, *Basic Semiconductor Physics*, Graduate Texts in Physics (Springer, Cham, 2017).
- [71] A. Kandus and C. G. Tsagas, *Mon. Not. R. Astron. Soc.* **385**, 883 (2008).
- [72] E. G. Blackman and G. B. Field, *Phys. Rev. Lett.* **71**, 3481 (1993).

- [73] N. Bessho and A. Bhattacharjee, *Phys. Plasmas* **14**, 056503 (2007).
- [74] L. P. Pitaevskii and E. M. Lifshitz, *Physical Kinetics: Volume 10 (Course of Theoretical Physics)* (Butterworth-Heinemann Ltd., Oxford, 1981).
- [75] A. Harutyunyan and A. Sedrakian, *Phys. Rev. C* **94**, 025805 (2016).
- [76] K. Tuchin, *J. Phys. G* **39**, 025010 (2012).
- [77] K. Hattori and D. Satow, *Phys. Rev. D* **94**, 114032 (2016).
- [78] Koichi Hattori, Shiyong Li, Daisuke Satow, and Ho-Ung Yee, *Phys. Rev. D* **95**, 076008 (2017).
- [79] K. Hattori, Xu-Guang Huang, D. H. Rischke, and D. Satow, *Phys. Rev. D* **96**, 094009 (2017).
- [80] M. Kurian and V. Chandra, *Phys. Rev. D* **99**, 116018 (2019).
- [81] B. Feng, *Phys. Rev. D* **96**, 036009 (2017).
- [82] P. Braun-Munzinger, K. Redlich, and J. Stachel, *Quark Gluon Plasma*, edited by R. C. Hwa *et al.* (World Scientific, Singapore, 2004), pp. 491–599.
- [83] A. Andronic, P. Braun-Munzinger, and J. Stachel, *Nucl. Phys. A* **772**, 167 (2006).
- [84] P. Braun-Munzinger, D. Magestro, K. Redlich, and J. Stachel, *Phys. Lett. B* **518**, 41 (2001); J. Cleymans and K. Redlich, *Phys. Rev. C* **60**, 054908 (1999); F. Becattini, J. Cleymans, A. Keränen, E. Suhonen, and K. Redlich, *Phys. Rev. C* **64**, 024901 (2001); J. Cleymans, B. Kampfer, M. Kaneta, S. Wheaton, and N. Xu, *Phys. Rev. C* **71**, 054901 (2005); A. Andronic, P. Braun-Munzinger, and J. Stachel, *Phys. Lett. B* **673**, 142 (2009).
- [85] R. Dashen, S. Ma, and H. J. Bernstein, *Phys. Rev.* **187**, 345 (1969).
- [86] R. Dashen and R. Rajaraman, *Phys. Rev. D* **10**, 694 (1974).
- [87] F. Karsch, K. Redlich, and A. Tawfik, *Phys. Lett. B* **571**, 67 (2003).
- [88] P. Braun-Munzinger, V. Koch, T. Schafer, and J. Stachel, *Phys. Rep.* **621**, 76 (2016).
- [89] M. Nahrgang, M. Bluhm, P. Alba, R. Bellwied, and C. Ratti, *Eur. Phys. J. C* **75**, 573 (2015).
- [90] A. Bhattacharyya, S. Das, S. K. Ghosh, R. Ray, and S. Samanta, *Phys. Rev. C* **90**, 034909 (2014).
- [91] R. K. Mohapatra, *Phys. Rev. C* **99**, 024902 (2019).
- [92] P. Garg, D. K. Mishra, P. K. Netrakanti, B. Mohanty, A. K. Mohanty, B. K. Singh, and N. Xu, *Phys. Lett. B* **726**, 691 (2013).
- [93] A. Bazavov *et al.*, *Phys. Rev. D* **86**, 034509 (2012).
- [94] V. V. Begun, M. I. Gorenstein, M. Hauer, V. P. Konchakovski, and O. S. Zozulya, *Phys. Rev. C* **74**, 044903 (2006).
- [95] D. H. Rischke, M. I. Gorenstein, H. Stocker, and W. Greiner, *Z. Phys. C* **51**, 485 (1991).
- [96] M. Albright and J. I. Kapusta, *Phys. Rev. C* **93**, 014903 (2016).
- [97] P. Deb, G. Kadam, and H. Mishra, *Phys. Rev. D* **94**, 094002 (2016).
- [98] J. Dey, S. Satapathy, P. Murmu, and S. Ghosh, [arXiv:1907.11164](https://arxiv.org/abs/1907.11164).
- [99] J. Dey, S. Satapathy, A. Mishra, S. Paul, and S. Ghosh, [arXiv:1908.04335](https://arxiv.org/abs/1908.04335).
- [100] S. Satapathy, S. Paul, A. Anand, R. Kumar, and S. Ghosh, [arXiv:1908.04330](https://arxiv.org/abs/1908.04330).
- [101] P. Mohanty, A. Dash, and V. Roy, *Eur. Phys. J. A* **55**, 35 (2019).
- [102] G. S. Denicol, Xu-Guang Huang, E. Molnr, G. M. Monteiro, H. Niemi, J. Noronha, D. H. Rischke, and Q. Wang, *Phys. Rev. D* **98**, 076009 (2018).
- [103] G. S. Denicol, E. Molnr, H. Niemi, and D. H. Rischke, *Phys. Rev. D* **99**, 056017 (2019).
- [104] A. Majumder and B. Muller, *Phys. Rev. Lett.* **105**, 252002 (2010).
- [105] G. Kadam, H. Mishra, and L. Thakur, *Phys. Rev. D* **98**, 114001 (2018).
- [106] P. Gondolo and G. Gelmini, *Nucl. Phys.* **B360**, 145 (1991).
- [107] C. Amsler *et al.* (Particle Data Group), *Phys. Lett. B* **667**, 1 (2008).
- [108] M. Albright, J. Kapusta, and C. Young, *Phys. Rev. C* **90**, 024915 (2014).
- [109] P. Braun-Munzinger, I. Heppe, and J. Stachel, *Phys. Lett. B* **465**, 15 (1999).